Article

Developmental Cell

Prior Fc receptor activation primes macrophages for increased sensitivity to IgG via long-term and short-term mechanisms

Graphical abstract

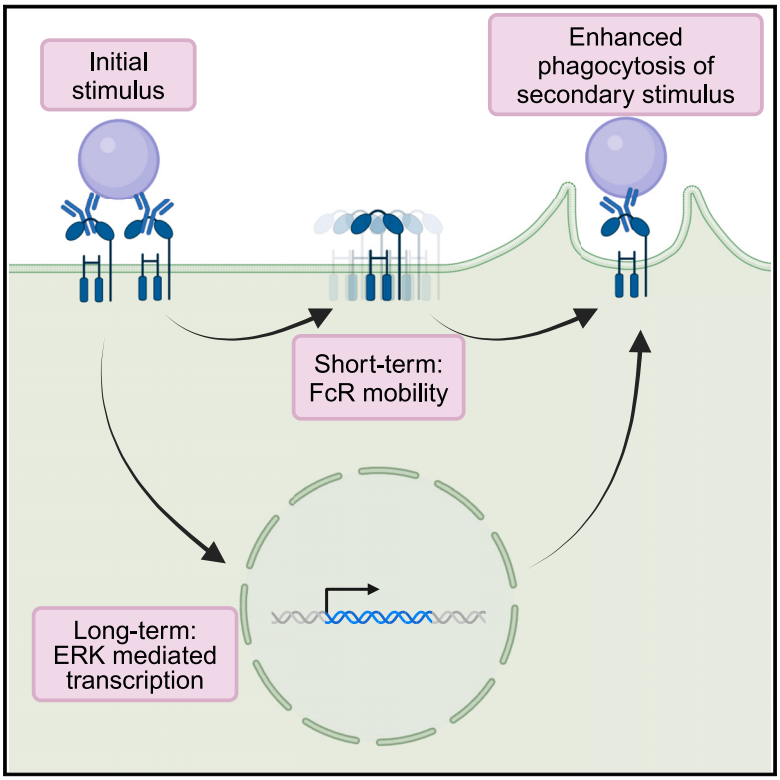

Authors

Annalise Bond, Sareen Fiaz, Kirstin Rollins, ..., Siddharth S. Dey, Maxwell Z. Wilson, Meghan A. Morrissey

Correspondence

morrissey@ucsb.edu

In brief

Bond et al. use optogenetics to show that prior subthreshold Fc receptor activation increases the phagocytosis of future antibody-opsonized targets. This priming response lasts at least 72 h and is associated with increased FcR mobility in the short term and Erk-mediated transcriptional changes in the long term.

Highlights

- Oligomerization of FcR-ITAM domains is sufficient to trigger phagocytosis
- Prior subthreshold activation of FcRs enhances antibody-dependent phagocytosis
- FcR activation increases FcR mobility within 1 h
- FcR activation increases phagocytosis for days by changing gene expression via Erk

Bond et al., 2024, Developmental Cell *59*, 1–15
November 4, 2024 © 2024 The Author(s). Published by Elsevier Inc.
https://doi.org/10.1016/j.devcel.2024.07.017

CellPress

Please cite this article in press as: Bond et al., Prior Fc receptor activation primes macrophages for increased sensitivity to IgG via long-term and short-term mechanisms, Developmental Cell (2024), https://doi.org/10.1016/j.devcel.2024.07.017

Developmental Cell

CellPress
OPEN ACCESS

Article

Prior Fc receptor activation primes macrophages for increased sensitivity to IgG via long-term and short-term mechanisms

Annalise Bond,[1] Sareen Fiaz,[1] Kirstin Rollins,[1] Jazz Elaiza Q. Nario,[1] Erika T. Snyder,[2] Dixon J. Atkins,[2] Samuel J. Rosen,[2] Alyssa Granados,[1] Siddharth S. Dey,[3,4] Maxwell Z. Wilson,[1] and Meghan A. Morrissey[1,5,*]

[1]Molecular Cellular and Developmental Biology Department, University of California, Santa Barbara, Santa Barbara, CA, USA
[2]Biomolecular Science and Engineering, University of California, Santa Barbara, Santa Barbara, CA, USA
[3]Chemical Engineering Department, University of California, Santa Barbara, Santa Barbara, CA, USA
[4]Bioengineering Department, University of California, Santa Barbara, Santa Barbara, CA, USA
[5]Lead contact
*Correspondence: morrissey@ucsb.edu
https://doi.org/10.1016/j.devcel.2024.07.017

SUMMARY

Macrophages measure the "eat-me" signal immunoglobulin G (IgG) to identify targets for phagocytosis. We tested whether prior encounters with IgG influence macrophage appetite. IgG is recognized by the Fc receptor. To temporally control Fc receptor activation, we engineered an Fc receptor that is activated by the light-induced oligomerization of Cry2, triggering phagocytosis. Using this tool, we demonstrate that subthreshold Fc receptor activation primes mouse bone-marrow-derived macrophages to be more sensitive to IgG in future encounters. Macrophages that have previously experienced subthreshold Fc receptor activation eat more IgG-bound human cancer cells. Increased phagocytosis occurs by two discrete mechanisms—a short- and long-term priming. Long-term priming requires new protein synthesis and Erk activity. Short-term priming does not require new protein synthesis and correlates with an increase in Fc receptor mobility. Our work demonstrates that IgG primes macrophages for increased phagocytosis, suggesting that therapeutic antibodies may become more effective after initial priming doses.

INTRODUCTION

Macrophages eat pathogens and infected, cancerous, or dying cells via phagocytosis. To select targets for phagocytosis, macrophages measure "eat-me" signals, like immunoglobulin G (IgG) antibodies. IgG is recognized by the Fc receptor (FcR), which is phosphorylated and recruits the kinase Syk, triggering downstream signaling.[1,2] Therapeutic IgGs like rituximab or trastuzumab trigger antibody-dependent cellular phagocytosis (ADCP) or antibody-dependent cellular cytotoxicity (ADCC) to reduce cancer growth.[2–7] Even many antibodies originally designed to block the function of their target actually activate the FcR for full efficacy.[8,9] Given the therapeutic importance, there is substantial interest in understanding how to boost macrophage phagocytosis.

What affects macrophage appetite? One important parameter is how sensitive a macrophage is to "eat-me" signals. Antibody-dependent phagocytosis requires the coordinated activation of a sufficient number of FcRs.[10] Targets with a subthreshold amount of IgG are not phagocytosed, despite triggering the initial steps in the phagocytosis signaling pathway.[10] In other macrophage signaling pathways, low levels of activating signal do not elicit any response on their own, but prime macrophages for rapid and intense response to future stimuli.[11] Whether subthreshold FcR signaling has any effect on macrophage appetite is not clear.

During an immune response or treatment with a therapeutic antibody, macrophages encounter multiple potential targets for phagocytosis sequentially, leading to bursts of FcR activation. Some encounters with antibody-opsonized cells result in phagocytosis of the entire cell,[3,5] but many cells do not have sufficient antibodies to trigger phagocytosis. Instead, macrophages may trogocytose, or nibble, a target cell or simply ignore it.[12–15] In some circumstances, prior phagocytosis increases macrophage appetite.[16,17] In contrast, other studies demonstrated that phagocytosing several whole cancer cells reduces macrophage appetite.[18] There is no clear, unifying model explaining these differences, which could be dependent on the specific "eat-me" signal presented, the time since phagocytosis, the intensity of the "eat-me" signal, digestion of the internalized particle, or any number of other factors.[19]

To unravel how prior IgG exposure affects macrophage appetite, we need to precisely control the timing and intensity of activating specific phagocytic receptors. Delivering a temporally controlled, homogeneous antibody stimuli to a population of cells is very difficult with the current tools. Because soluble IgG does not activate the FcR, IgG must be presented on

This is an open access article under the CC BY license (http://creativecommons.org/licenses/by/4.0/).

Please cite this article in press as: Bond et al., Prior Fc receptor activation primes macrophages for increased sensitivity to IgG via long-term and short-term mechanisms, Developmental Cell (2024), https://doi.org/10.1016/j.devcel.2024.07.017

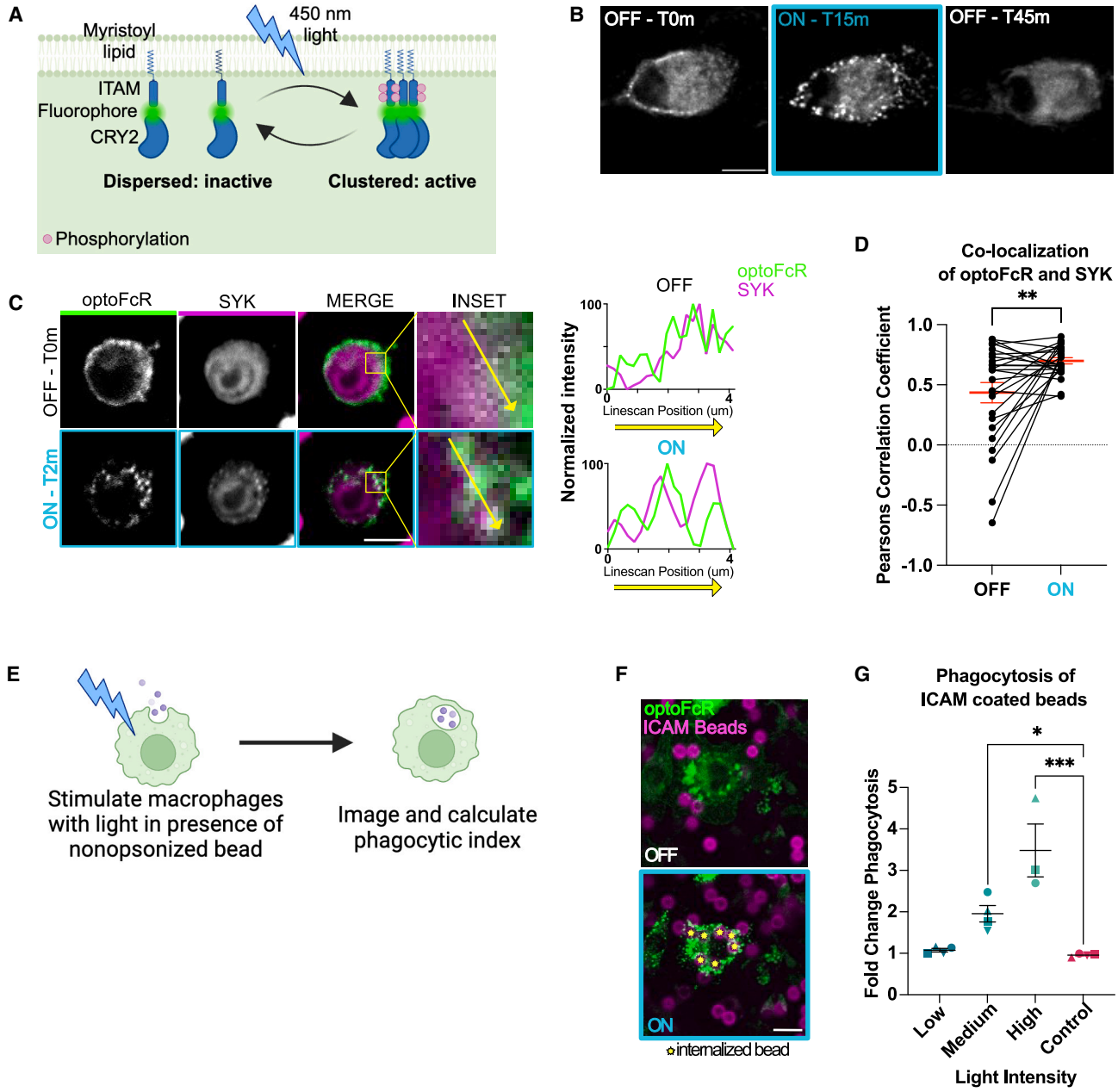

Figure 1. Optogenetic Fc receptor controls phagocytosis

(A) Schematic of optogenetic Fc receptor (optoFcR) design, containing a myristoylation signal for membrane localization, the ITAM-containing intracellular domain from the FcR gamma-chain for signaling, mScarlet fluorophore, and the homo-oligomerizing peptide—cryptochrome 2 (CRY2olig).

(B) The optoFcR in bone-marrow-derived macrophages (BMDMs) starts dispersed on the membrane (T0m; $n = 0/22$ cells with visible clusters) and clusters after 15 min of constant, high-intensity light (T15m; $n = 21/22$ cells with visible clusters). The optoFcR is declustered after 30 min in the dark (T45m; $n = 0/22$ cells with visible clusters). See also Video S1.

(C) The downstream effector protein, Syk, colocalized with optoFcR in Raw264.7 macrophages stably expressing both the optoFcR and Syk-mNeonGreen. A line scan (right) shows the Syk and optoFcR intensity at the position indicated by the yellow arrow in the inset. See also Video S2.

(D) Graph shows the Pearson's correlation coefficient for Syk and optoFcR at the cell cortex. Each data point represents a region of interest (ROI) drawn around a membrane region of a cell. The same ROI was used for both T0 (OFF) and T2 (ON), and the data points from the same ROI are connected by a line.

(E) Schematic of experimental design for (F) and (G).

(F) OptoFcR-expressing (green) macrophages and ICAM-conjugated beads are visualized by atto390 in the supported lipid bilayer (magenta) before (OFF) and after (ON) 15 min of optoFcR activation with high-intensity light. Internalized beads are labeled with a yellow star. See also Video S3.

(legend continued on next page)

Please cite this article in press as: Bond et al., Prior Fc receptor activation primes macrophages for increased sensitivity to IgG via long-term and short-term mechanisms, Developmental Cell (2024), https://doi.org/10.1016/j.devcel.2024.07.017

CellPress
OPEN ACCESS

antibody-bound targets. Controlling precisely the number of targets a macrophage encounters, or the timing of these encounters, is very difficult and low throughput.

To quantitatively control the duration and strength of FcR activation, we developed an optogenetic FcR (optoFcR). We found that prior FcR activation primes macrophages for greater responses to subsequent stimuli. Counterintuitively, low levels of optoFcR activation induced stronger priming than high levels of optoFcR activation. Macrophage priming is controlled by two independent mechanisms, one short-term (<1 h) and one long-term response (starting at 4 h and lasting up to 3 days). The short-term response is associated with an increase in FcR mobility, accelerated initiation of phagocytosis, and increased phagocytic cup formation. The long-term response requires activation of Erk to drive a transcriptional response that leads to increases in both initiation and completion of phagocytosis. These data suggest that macrophages can integrate signaling from previous encounters with IgG to modify the response to the next target. This study provides insight into how macrophage appetite is regulated and may suggest strategies to enhance ADCP.

RESULTS

OptoFcR recapitulates native FcR signaling for precise temporal control over signaling

To precisely control the temporal pattern of FcR activation across an entire field of cells, we sought to design an optoFcR that could be turned on and off with light. Prior work has shown that the FcR clusters upon IgG binding. Although the FcR has no inherent kinase activity, clustering promotes phosphorylation of the intracellular immunoreceptor tyrosine-based activation motifs (ITAMs) and phagocytosis.[20–22] We hypothesized that clustering may be sufficient to induce FcR activation. To test this, we designed an optoFcR construct that consists of a myristoylation sequence for membrane localization, the intracellular domain for the native FcR ɣ-chain and a light-activatable peptide CRY2 (Figure 1A). We selected the variant CRY2olig because it forms multimeric, rapidly reversible clusters.[23] Upon blue light (450 nm) stimulation the optoFcR oligomerizes (Figure 1B; Video S1). Clusters dissociate when the cells are returned to the dark (Figure 1B). Like the native FcR when it is bound to IgG, the optoFcR clusters increased in size and number with more light stimulation and partially excluded CD45 (Figures S1A–S1F). Clustering also results in the recruitment of the downstream effector protein Syk, suggesting that clustering is sufficient to induce FcR phosphorylation (Figures 1C and 1D; Video S2).

We next sought to determine whether clustering of the optoFcR is sufficient to trigger phagocytosis. We incubated ICAM-1-conjugated beads with macrophages expressing either the optoFcR or membrane-tethered mCherry (mCh-CAAX) and exposed them to 15 min of light stimulation (Figure 1E). ICAM-1 mediates bead binding to the macrophage, but does not trigger phagocytosis of otherwise unopsonized beads.[24,25] Macrophages expressing the optoFcR engulfed three times as many beads as control macrophages when stimulated with the highest intensity light and twice as many beads when stimulated with medium intensity light (Figures 1F and 1G; Video S3). Low-intensity light did not activate phagocytosis. This dose response is similar to the dose response seen in IgG-mediated phagocytosis (Figures S1G and S1H). Together, these data demonstrate that clustering of the FcR-ITAM domain is sufficient to initiate phagocytosis in macrophages without a specific "eat-me" signal.

Prior FcR activation enhances the phagocytosis of IgG-coated beads

With the ability to temporally control FcR activation in bone-marrow-derived macrophages (BMDMs), we next sought to determine whether prior FcR activation influences phagocytic ability. We stimulated macrophages with low-intensity blue light to activate the optoFcR for 15 min, which is around the same timescale that a macrophage interacts with a phagocytic target. We then waited 1 or 12 h before adding IgG-opsonized beads, which is sufficient time for the optoFcR to completely decluster. Then we measured the number of beads engulfed per cell using microscopy (Figure 2A). We found that prior optoFcR activation increased the amount of eating roughly 2-fold compared with cells that either did not receive prior light stimulation or did not express the optoFcR (Figure 2B). This demonstrates that prior FcR activation primes macrophages to respond to future IgG.

Next, we systematically varied the light intensity and stimulation time used to activate the optoFcR as well as the delay between activating the optoFcR and measuring phagocytosis of IgG-coated beads. In all cases, we found that low doses of light, and thus less FcR activity, led to the highest macrophage priming (Figures 2C and 2D). The amount of light that best primed macrophages was not sufficient to activate phagocytosis on its own (Figure 1G). None of the conditions we tested changed the surface expression of activating or inhibiting FcRs or the inhibitory receptor SIRPa (Figures S2A–S2E). Together, this suggests that a subthreshold level of FcR activation, not sufficient to activate phagocytosis, primes macrophages for future encounters with IgG.

We then wanted to know whether we could induce macrophage priming using IgG and the endogenous FcR. Based on our data from the optoFcR, we predicted that a low level of IgG exposure would enhance phagocytosis of a second dose of IgG-coated beads. To test this, we preincubated macrophages with beads containing an IgG density that did not activate phagocytosis (Figure S1) or with unopsonized beads. We then extensively washed the macrophages to remove these beads and added a second color of IgG-bound beads (Figure 2E). We found that macrophages preincubated with IgG-coated beads phagocytosed more than macrophages preincubated with unopsonized beads when the second dose was above the threshold for inducing phagocytosis (Figures 2F and S2F). This suggests that the native IgG and FcR system primes macrophages like the optoFcR system.

(G) Quantification of phagocytosis in BMDMs after 15 min of optoFcR stimulation at low (5 μW/cm^2), medium (90 μW/cm^2), and high (1,390 μW/cm^2) intensity light compared with control cells that do not express the optoFcR but receive the high-intensity light stimulus. Each data point represents the mean of an independent experiment. Data collected in the same replicate are denoted by symbol shape. In all graphs, bars represent the mean ±SEM. *indicates $p < 0.05$, ***indicates $p < 0.0005$ using a paired t test (D), one-way ANOVA with Dunnett correction (G). Scale bars are 10 μm.
See also Figure S1 and Videos S1, S2, and S3.

Please cite this article in press as: Bond et al., Prior Fc receptor activation primes macrophages for increased sensitivity to IgG via long-term and short-term mechanisms, Developmental Cell (2024), https://doi.org/10.1016/j.devcel.2024.07.017

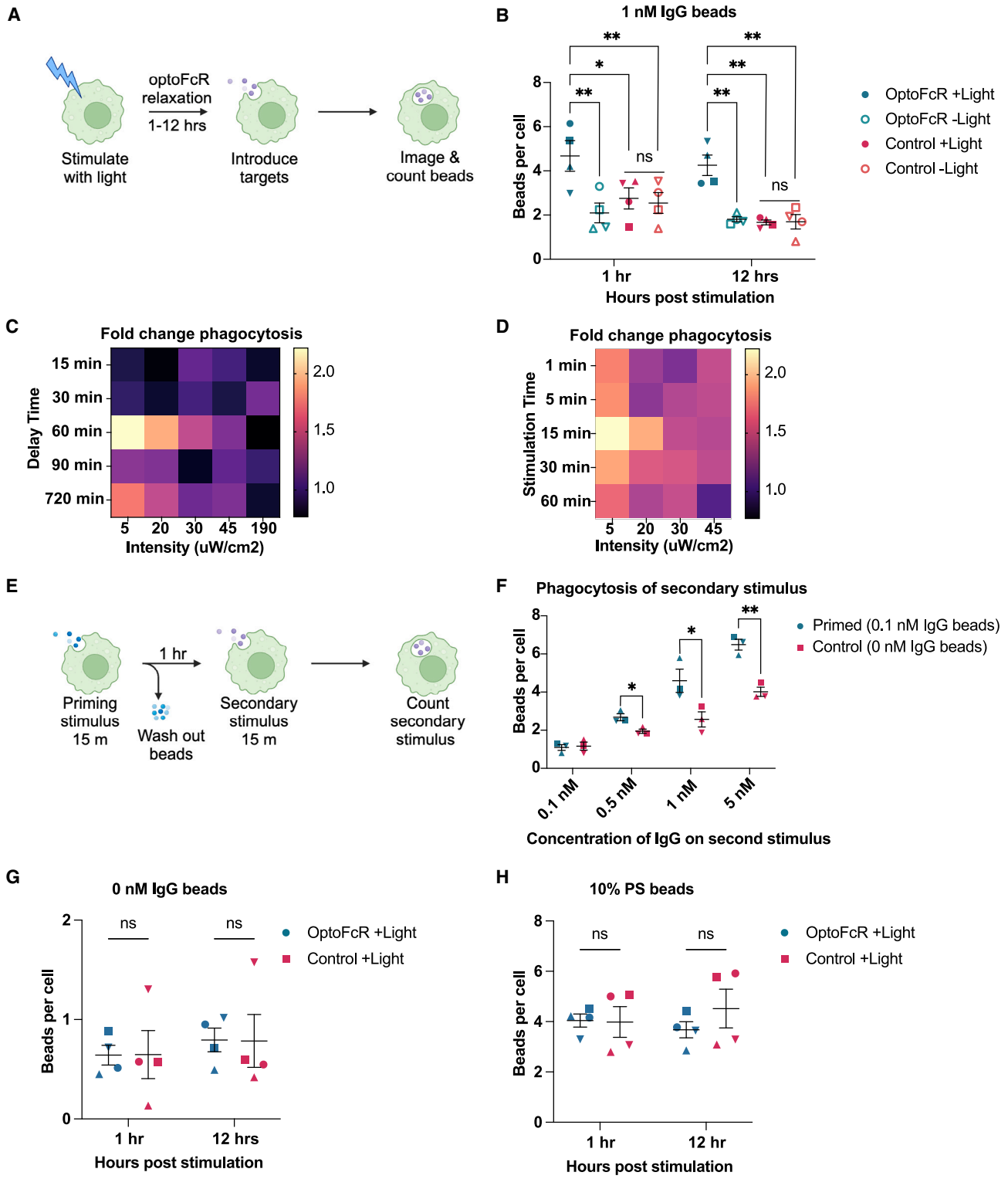

Figure 2. Prior FcR activation specifically enhances macrophage sensitivity to IgG

(A) Schematic of experimental design for light-induced priming. Control (mCherry-CAAX) and optoFcR-expressing BMDMs were stimulated with light for 15 min. The cells were returned to the dark for either 1 or 12 h, and then targets opsonized with 1 nM IgG (approx. 10–18 IgG molecules/μm^2) were introduced. After 15 min of phagocytosis, beads were washed out. Cells were imaged and the number of targets phagocytosed per cell was counted.

(B) Quantification of experiment described in (A). OptoFcR-expressing cells that received light phagocytosed significantly more than cells that did not receive light, or cells that received light but did not express the optoFcR.

(legend continued on next page)

Please cite this article in press as: Bond et al., Prior Fc receptor activation primes macrophages for increased sensitivity to IgG via long-term and short-term mechanisms, Developmental Cell (2024), https://doi.org/10.1016/j.devcel.2024.07.017

CellPress
OPEN ACCESS

Prior FcR activation specifically enhances the phagocytosis of IgG-coated beads, not PS or unopsonized beads

We next wanted to know whether prior FcR activation specifically primed macrophages to phagocytose IgG-coated targets or whether it broadly enhanced phagocytosis. We first determined whether prior optoFcR activation increased non-specific phagocytosis of unopsonized targets. Primed macrophages did not phagocytose more unopsonized beads than control macrophages (Figure 2G). We then determined whether prior optoFcR activation increased efferocytosis, the engulfment of apoptotic cells. The molecular regulators of efferocytosis partially overlap with antibody-dependent phagocytosis, but the processes require some unique signaling pathways, including different "eat-me" signal receptors.[26] By integrating phosphatidylserine (PS), an efferocytic "eat-me" signal, into the lipid mixture on our silica bead targets, we can recapitulate apoptotic corpse engulfment *in vitro*.[27] We incubated PS-coated beads with macrophages at 1 and 12 h post light stimulation and measured the amount of eating. There was no change in the amount of eating at either time point (Figure 2H). These data suggest that prior FcR activation primes macrophages to specifically react to IgG. This also suggests that the molecular regulators of priming are unique to FcR signaling rather than in one of the pathways shared by efferocytosis and antibody-dependent phagocytosis.

We then investigated whether prior FcR stimulation changed macrophage sensitivity for IgG, lowering the threshold of IgG required for initiating phagocytosis. Alternatively, priming could increase macrophage capacity—the maximum number of targets each macrophage can engulf. To do this, we added beads with various concentrations of IgG to BMDMs and calculated the fold change in phagocytosis (Figures S2G and 2H). Primed macrophages show enhanced eating of beads with low concentration of IgG. The total capacity for phagocytosis is not significantly changed in primed macrophages. This indicates that priming primarily alters macrophage sensitivity to low levels of IgG, rather than overall capacity for phagocytosis.

Primed macrophages phagocytose more antibody-opsonized cancer cells

We next sought to determine whether primed macrophages can increase whole-cell eating of opsonized cancer cell targets. In addition to phagocytosis, macrophages often trogocytose or nibble target cells, stripping the cancer cells of target antigen without killing them.[15] Prior clinical studies have shown that the anti-CD20 therapeutic antibody (rituximab) is most effective when administered more frequently at a low dose, which minimizes antigen shaving.[28] Given our results, we hypothesized that prior FcR activation might also enhance phagocytosis of cancer cells. We first measured phagocytosis of Raji B cells incubated with increasing concentrations of anti-CD20 antibody to find an antibody concentration where we could detect a change in macrophage sensitivity (Figures S3A and S3B). To measure both the amount of whole-cell phagocytosis and trogocytosis, we incubated IgG-opsonized Raji cell targets with primed or unprimed optoFcR-expressing BMDMs and analyzed the cells with timelapse microscopy (Figures 3A and 3B; Video S4). We found that the number of Raji cells phagocytosed and the percentage of phagocytic macrophages increased in primed macrophages (Figures 3C and 3D). The percentage of primed macrophages that trogocytosed was not significantly increased compared with unprimed macrophages (Figure 3E). This suggests that primed macrophages are better at phagocytosing antibody-opsonized cancer cells.

We then took the experiment a step further and asked whether antibody-opsonized cancer cells could prime macrophages via the endogenous FcR. We incubated macrophages with either opsonized or unopsonized Rajis for 15 min before washing out the Rajis. 24 h later, we added opsonized and fluorescently labeled Rajis to all conditions and measured phagocytosis and trogocytosis by timelapse microscopy (Figures 3F and 3G; Video S5). We found that the endogenous system primed macrophages for more whole-cell eating (Figures 3H–3J). In contrast, trogocytosis in primed macrophages was fairly similar to unprimed macrophages (Figure 3I). Priming macrophages via the endogenous IgG-FcR system increased phagocytosis even more than priming with the optoFcR system. These data suggest that prior exposure to antibody-opsonized cancer cells increases phagocytosis at low IgG densities.

Macrophage priming occurs through a short-term and long-term mechanism

We next sought to determine the molecular mechanism for enhanced phagocytosis after FcR activation. We observed enhanced phagocytosis at both 1 and 12 h after optoFcR stimulation (Figure 2B). Although 12 h post stimulation is likely enough time for changes in transcription or translation to affect macrophage phenotypes, 1 h is likely too short for this mechanism.

(C and D) Heatmaps of fold change in phagocytosis of 1 nM IgG beads in optoFcR-expressing macrophages that received a priming dose of light compared with optoFcR-expressing macrophages that did not receive light stimulation. In (C) the intensity and delay time between initial stimulation and bead addition were altered. In (D) the priming dose of light and stimulation time were altered. Data are from 2 independent replicates.

(E) Schematic of experimental design for priming macrophages with IgG beads. Wild-type BMDMs were given either beads with 0.1 or 0 nM IgG for 15 min as a priming stimulus. Those beads were then washed out and the cells were allowed to recover for 1 h. A second set of different color beads ligated to IgG at the indicated concentration were added and the amount of phagocytosis was determined after 15 min.

(F) Quantification of phagocytosis for experiment described in (E). Macrophages that were preincubated with 0.1 nM IgG-conjugated beads phagocytosed significantly more than macrophages preincubated with unopsonized beads.

(G) Phagocytosis of bead targets without an "eat-me" signal. Experiment was performed as described in (A) except the beads did not contain IgG.

(H) Phagocytosis of bead targets with the efferocytic "eat-me" signal, phosphatidylserine. Experiment was performed as described in (A) except the beads were covered in a 10% phosphatidylserine bilayer to mimic an apoptotic corpse.

In all graphs, each point represents the mean of an independent experiment. Data collected in the same replicate are denoted by symbol shape. Bars represent the mean ± SEM. *indicates $p < 0.05$, **indicates $p < 0.005$, ****indicates $p < 0.0001$ by two-way ANOVA with Sidak corrections (B), multiple t tests with Holm-Sidak corrections (F), and unpaired t test (G) and (H).

See also Figure S2.

Please cite this article in press as: Bond et al., Prior Fc receptor activation primes macrophages for increased sensitivity to IgG via long-term and short-term mechanisms, Developmental Cell (2024), https://doi.org/10.1016/j.devcel.2024.07.017

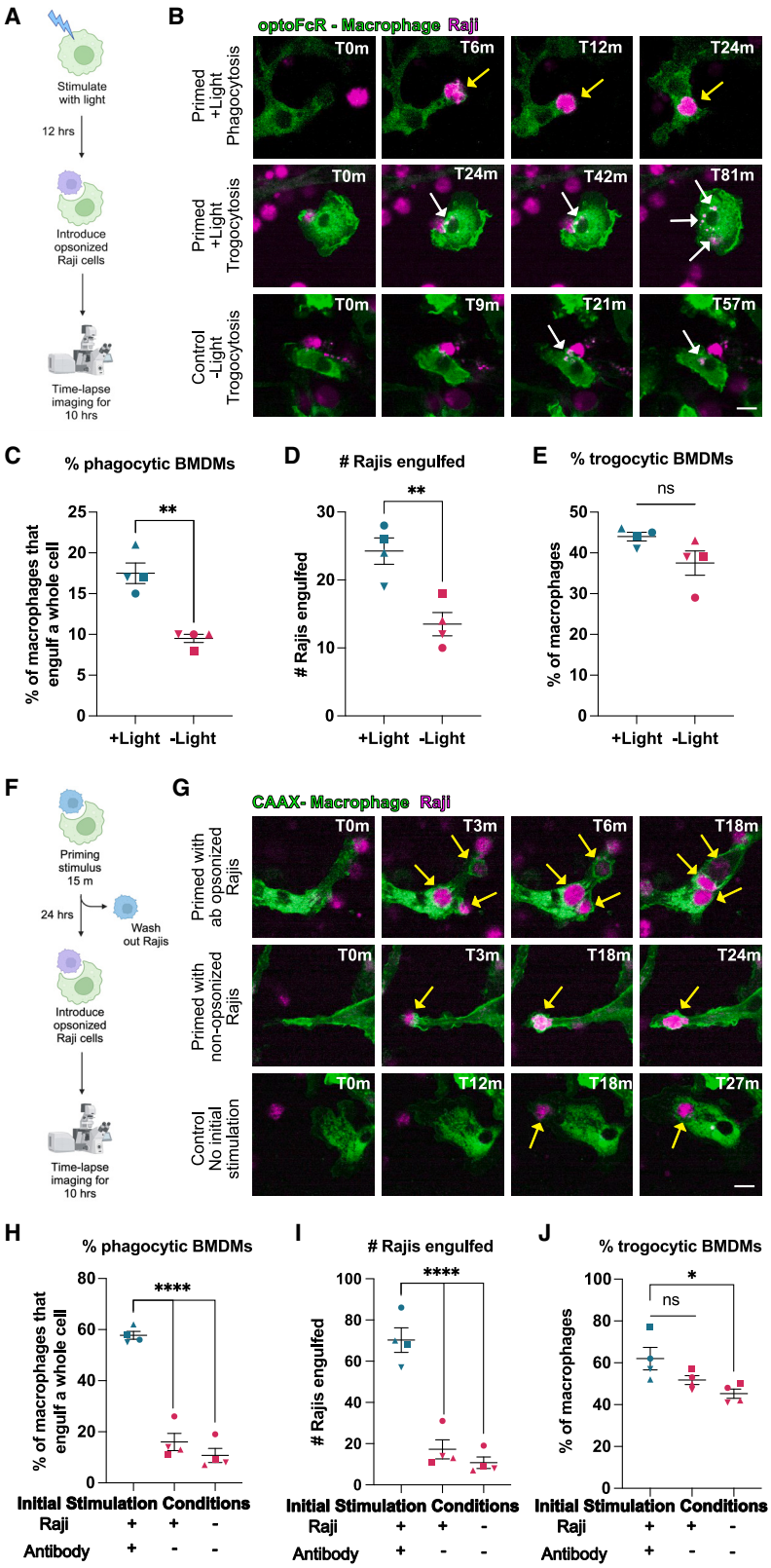

Figure 3. Macrophages are primed for increased cancer cell engulfment

(A) Schematic of experimental design for priming with optoFcR and secondary stimulation with cancer cell targets. OptoFcR cells were exposed to light for 15 min, then returned to the dark. Raji B cells opsonized with 5 ng/mL IgG were added after 12 h, and the cancer cell-macrophage interactions were captured by timelapse microscopy.

(B) OptoFcR-expressing (mSc; green) macrophages phagocytosed and trogocytosed Raji B cells (CellTrace far red; magenta). Yellow arrows point to phagocytosis of a whole cancer cell and white arrows point to trogocytosis of cancer cell fragments. See also Video S4.

(C) Percent of BMDMs that engulfed a whole target cell increased with prior FcR stimulation.

(D) The number of whole Raji B cells engulfed was greater in primed macrophages.

(E) Percent of BMDMs that trogocytosed a target was not significantly different with priming.

(F) Schematic of experimental design for priming and secondary stimulation with cancer cell targets. BMDMs were primed with opsonized (5 ng/mL IgG) or unopsonized Raji B cells for 15 min before Raji B cells were washed out. After 14 h, a second stimulation of Raji B cells opsonized with 5 ng/mL IgG were introduced and cancer cell-macrophage interactions were imaged with timelapse microscopy.

(G) Representative images of phagocytosis in each of the three conditions. Raji B cells were visualized using CellTrace far red (magenta) and BMDMs were visualized with CAAX-mCh expression (green). Yellow arrows denote phagocytosis of a whole cancer cell. See also Video S5.

(H) The percentage of BMDMs that engulfed a Raji target increased with prior stimulation with opsonized targets compared with stimulation with unopsonized targets or no prior stimulation.

(I) The number of whole Raji targets engulfed was greater in primed macrophages.

(J) The percent of BMDMs that trogocytosed was similar in primed macrophages compared with controls.

Each data point represents the mean of an independent experiment, denoted by symbol shape, and bars represent the mean ± SEM. *indicates $p < 0.05$, **indicates $p < 0.005$, ****indicates $p < 0.0001$ using an unpaired t test (C)–(E) or one-way ANOVA with Sidak corrections.

See also Figure S3 and Videos S4 and S5.

Please cite this article in press as: Bond et al., Prior Fc receptor activation primes macrophages for increased sensitivity to IgG via long-term and short-term mechanisms, Developmental Cell (2024), https://doi.org/10.1016/j.devcel.2024.07.017

CellPress
OPEN ACCESS

We decided to carefully assay when macrophage priming occurred. To do this, we activated the optoFcR and varied the time before presenting a second stimulus of IgG-coated beads and measuring phagocytosis. We saw robust priming occurring in two discrete waves: a short-term response that peaks around 1 h after FcR activation and a long-term response that begins at 4 h after FcR activation and persists for at least 72 h (Figure 4A).

As the long-term priming following optoFcR activation persists for at least 72 h, we speculated that this response requires *de novo* protein production rather than a more transient post-translational modification mechanism. We evaluated priming in macrophages treated with cycloheximide (CHX) and actinomycin D (AD) to inhibit translation and transcription, respectively. Treatment with either CHX or AD significantly reduced phagocytosis in primed macrophages compared with DMSO treated control macrophages at 4 and 6 h post light stimulation (Figure 4B). This suggests that *de novo* mRNA and protein synthesis is required for a long-term memory response. Blocking new protein synthesis did not significantly reduce priming at 1 h post stimulation, suggesting that short-term memory is not reliant on new protein production (Figure 4B). Overall this suggests that there are two mechanisms for macrophage priming—one that operates on a short timescale and does not require synthesis of new proteins and one that operates on a long timescale and requires changes in gene expression.

Erk activation is required for long-term priming

Because long-term priming requires new protein production, we sought to dissect which transcriptional programs were being executed by the macrophages. Erk, a nuclear kinase, functions downstream of the FcR and regulates the macrophage dose-dependent response to lipopolysaccharides (LPS) as well as many other immune signaling pathways.[11] To determine whether Erk contributes to macrophage priming, we used PD0325901 to block Erk activity. We then stimulated the optoFcR for 15 min, waited 1 or 12 h, and measured phagocytosis of IgG-coated beads. Inhibiting Erk signaling blocked long-term memory with no effect on short-term memory (Figure 4C). These results indicate that long-term priming requires a transcriptional response mediated by Erk activation.

Prior FcR activation increases the expression of immune response genes

Because long-term priming requires changes in gene expression, we characterized the transcriptional profile of primed and unprimed macrophages using bulk RNA sequencing (RNA-seq). We found that differentially regulated genes were enriched for Gene Ontology (GO) annotations associated with immune response pathways (Figures 5A and S4A). We additionally assessed the polarization of primed macrophages compared with classically polarized M1 and M2 macrophages by RNA-seq. Primed macrophages resemble M2 polarized macrophages but have a unique transcriptional profile that does not fully recapitulate either M1 or M2 polarization (Figures 5B and S4B; Table S1).

Long-term macrophage priming increases both the frequency of initiating phagocytosis and the speed of completing phagocytosis

To further understand the effects of the transcriptional changes, we sought to isolate which step in the phagocytic process was enhanced by prior subthreshold activation of the FcR. To do this, we quantified the kinetics of engulfment using live cell imaging, breaking the process of phagocytosis into three steps: target binding, initiation of phagocytosis, and completion[21] (Figures 5C and 5D; Video S6). We then quantified the time between each step in primed and unprimed macrophages and the percent of bead contacts that successfully progressed from one step to the next without membrane retraction and target release. We also measured the percent of beads that were bound to macrophages but found no difference between primed and unprimed macrophages (Figure 5E). Primed macrophages were more likely to both initiate and complete phagocytosis and the time between initiation and completion was decreased (Figures 5F–5I). Additionally, the overall success of phagocytosis, from bead binding to completion, was roughly 2-fold higher in primed macrophages (Figure 5J). Stimulated control macrophages that do not express the optoFcR did not show a difference in any measure of phagocytosis compared with unstimulated control macrophages (Figures S4C–S4H). This suggests that the transcriptional changes that cause long-term priming are affecting phagocytic machinery involved in multiple stages of phagocytosis.

Short-term priming increases the speed and frequency of initiating phagocytosis

Having demonstrated that short-term priming does not require new protein synthesis like long-term priming, we sought to determine the mechanism for short-term priming. To do this, we repeated the kinetics experiment on cells 1 h after optoFcR activation (Figure 6A). Primed macrophages were more likely to bind beads and initiate phagocytosis, and the time between bead binding and initiation was less (Figures 6B–6D). The increase in bead binding did not correlate with a decrease in CD44 expression, a key protein regulating the pericellular matrix[29] (Figure S5B). In contrast, after initiation, the chance of successfully completing phagocytosis and the speed of phagocytosis were the same in primed and unprimed macrophages (Figures 6E and 6F). Overall, the percent of bead contacts that result in successful phagocytic events is significantly increased in primed macrophages (Figure 6F). Stimulated control macrophages that do not express the optoFcR did not show a difference in any measure of phagocytosis compared with unstimulated macrophages (Figures S5A–S5G). These data indicate that prior subthreshold FcR activation primes macrophages for faster target recognition and more frequent signal initiation, implicating early phagocytic machinery.

Priming is associated with enhanced FcR mobility

As initiation of phagocytosis is faster in primed macrophages, and our prior data indicated that the molecular regulator of priming was specific to the FcR pathway (Figures 2G and 2H), we decided to look at FcR mobility. Clustering of IgG, and subsequently FcR, increases the frequency and speed of initiating phagocytosis but not the speed of cup closure, similar to the phenotype we observed in our phagocytosis kinetics analysis.[21] FcR cluster formation and subsequent activation is dependent on the lateral mobility of FcRs, which is constrained by a heterogeneous F-actin "fence" and other mechanisms.[29–32] Increased FcR mobility correlates with increased binding of IgG-coated

Please cite this article in press as: Bond et al., Prior Fc receptor activation primes macrophages for increased sensitivity to IgG via long-term and short-term mechanisms, Developmental Cell (2024), https://doi.org/10.1016/j.devcel.2024.07.017

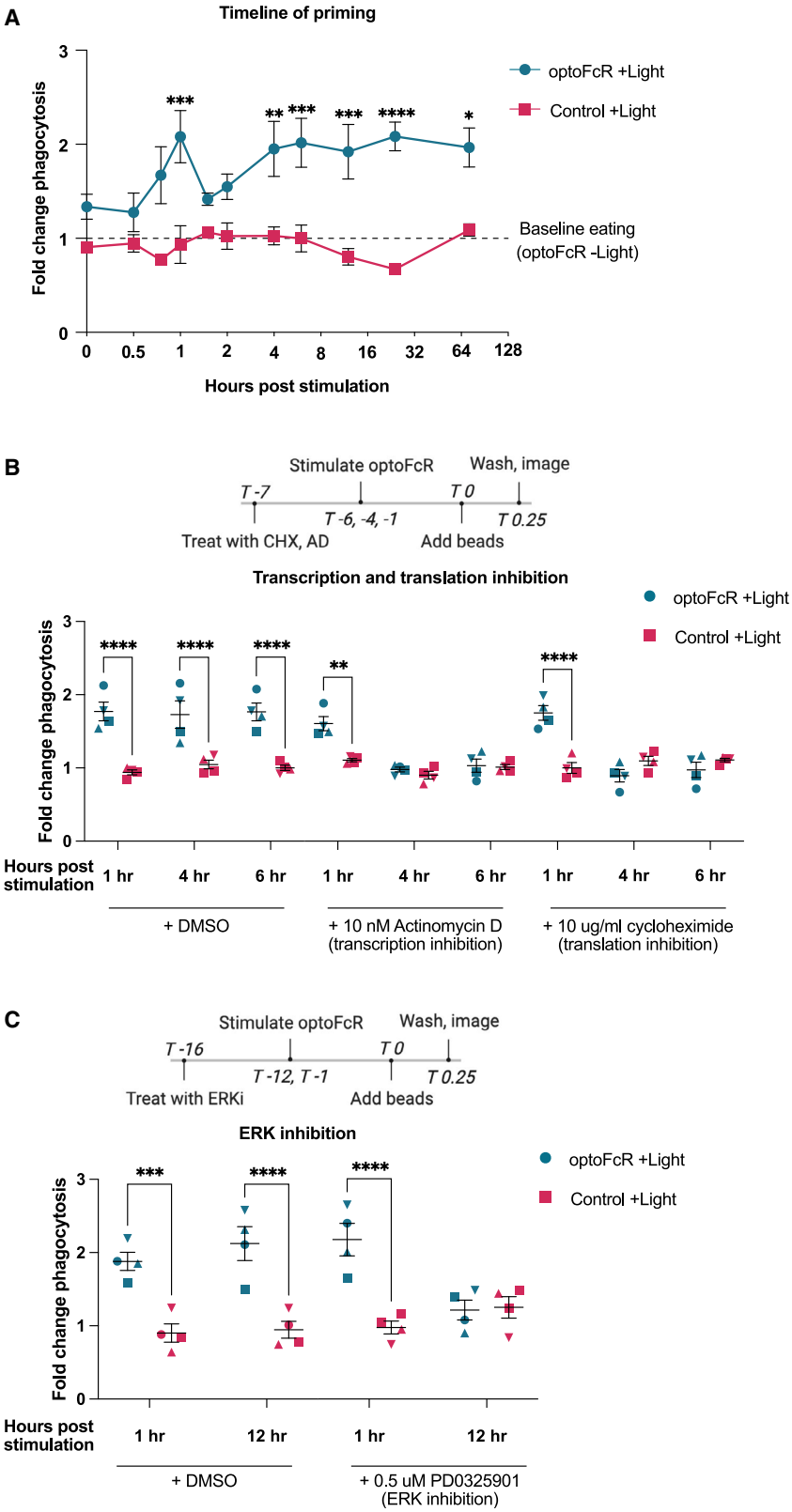

Figure 4. FcR-mediated priming occurs via a short- and long-term mechanism

(A) Phagocytosis of 1nM IgG beads added at the indicated time post 15 min low-intensity light stimulation for macrophages expressing the optoFcR (blue) or a control mCh-CAAX (red). Enhanced phagocytosis occurs in two discrete peaks and lasts for at least 72 h. Points denote the mean of 4 independent replicates. Phagocytosis is normalized to unstimulated control cells.

(B) Macrophages were treated with actinomycin D (AD, 10 nM) or cycloheximide (CHX, 10 μg/mL) to block transcription or translation, respectively, starting 7 h before phagocytosis. Macrophages were stimulated with light to activate the optoFcR at 1, 4, or 6 h before phagocytosis. AD and CHX did not eliminate priming at 1 h post stimulation. AD and CHX eliminated the enhanced phagocytosis phenotype at 4 and 6 h post stimulation.

(C) Macrophages were treated with Erk inhibitor (PD0325901, 0.5 μM) or DMSO control for 16 h before measuring phagocytosis. OptoFcR macrophages stimulated with light 1 h before bead addition still showed enhanced phagocytosis. Macrophages stimulated with light 12 h before bead addition phagocytosed the same number of beads as controls. Phagocytosis is normalized to unstimulated control cells.

Each data point represents the mean of an independent experiment. Data collected in the same replicate are denoted by symbol shape. Bars represent the mean ± SEM. *indicates $p < 0.05$, **indicates $p < 0.005$, ***indicates $p < 0.0005$, ****indicates $p < 0.0001$ using a two-way ANOVA with Sidak corrections (A)–(C).

Please cite this article in press as: Bond et al., Prior Fc receptor activation primes macrophages for increased sensitivity to IgG via long-term and short-term mechanisms, Developmental Cell (2024), https://doi.org/10.1016/j.devcel.2024.07.017

CellPress
OPEN ACCESS

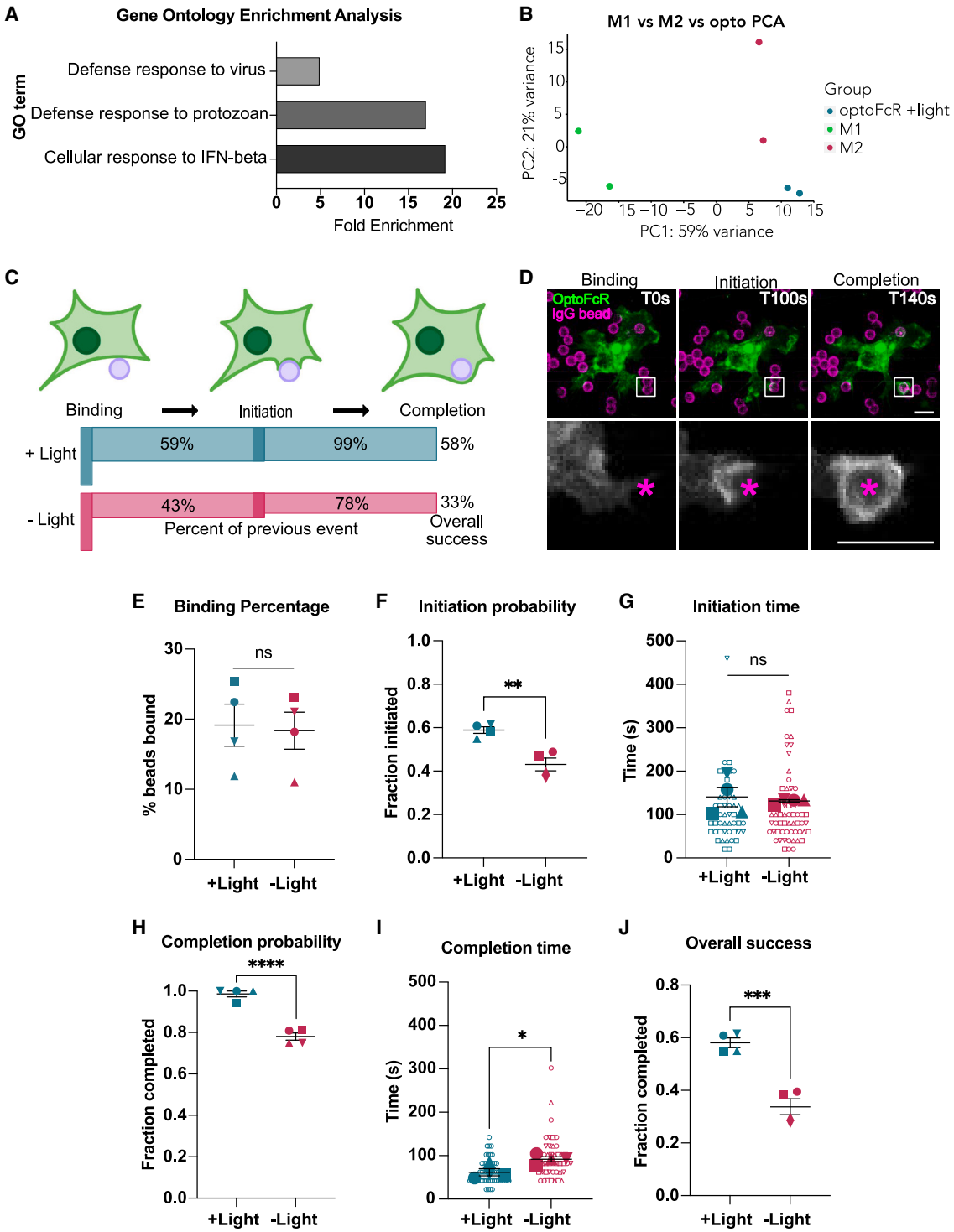

Figure 5. Transcriptional changes drive priming through an increase in both initiation and completion of phagocytosis

(A) GO analysis of genes that were greater than 1$\log_2$ fold differentially expressed in primed macrophages compared with both stimulated control macrophages (lentivirally infected with CAAX-mCh) and to unstimulated optoFcR macrophages. Only genes that were differentially expressed in both comparisons were included.

(B) PCA of primed macrophages gene expression profile compared with M1 polarized (stimulated with LPS and interferon [IFN]-γ) macrophages and M2 polarized (stimulated with interleukin [IL]-4) macrophages.

(C) OptoFcR macrophages received 15 min light stimulus 12 h before bead addition (primed) and were compared with optoFcR macrophages that did not receive light stimulation (unprimed). Timelapse imaging was used to quantify the kinetics of phagocytosis. Schematic shows each step in phagocytosis: binding (target

(legend continued on next page)

Please cite this article in press as: Bond et al., Prior Fc receptor activation primes macrophages for increased sensitivity to IgG via long-term and short-term mechanisms, Developmental Cell (2024), https://doi.org/10.1016/j.devcel.2024.07.017

targets and phagocytosis.[29,31,33] We hypothesized that primed macrophages may have higher FcR mobility, which could explain the increased speed and frequency of initiating phagocytosis. To determine whether optoFcR priming increases receptor mobility, we tracked single FcR molecules on optoFcR primed and unprimed cells (Figure 6H). On average, the FcR molecules on primed macrophages had a higher mean jump distance (MJD; average distance traveled between frames) than on unprimed macrophages (Figure 6I). Graphing the MJD of individual tracks, primed macrophages had a multi-modal distribution of track MJDs, suggesting there may be a more mobile population in the primed macrophages (Figure 6J).

Previous studies have described FcR motion as free or confined.[29,31] Confined FcRs have limited mobility and may not be available to form signaling microclusters required for phagocytosis. To see whether primed macrophages had more free FcRs, we categorized FcR tracks by motion type using a moment scaling spectrum (MSS) analysis. MSS categorizes modes of random motion and has previously been used to classify FcR motion types.[31] Consistent with previous studies, we found a population of confined FcRs that were restricted to small microdomains or "corals" within the membrane (Figures 6K and 6L).[29,31] This population decreased in primed macrophages, suggesting that more FcRs may be available to join signaling microclusters. In addition, the average diffusion coefficient, indicative of how far individual receptors travel, was significantly higher in primed macrophages (Figure 6M). Overall, these data suggest that there is an increase in the mobile fraction of FcRs on primed macrophages, which may increase formation of FcR signaling clusters and the probability of initiating phagocytosis.

DISCUSSION

Our work suggests that the macrophage response to IgG integrates information from sequential encounters with IgG-coated targets. Prior FcR activation makes macrophages more likely to phagocytose an IgG-coated target. This enhanced phagocytosis correlates with an increase in FcR mobility in the short term. Long-term priming requires Erk signaling and transcription of new proteins.

Clustering of the FcR has previously been linked to its activation and enhanced phagocytosis.[21,22,34,35] We recapitulate this clustering using an optogenetic method and find that clustering of the optoFcR is sufficient to drive Syk recruitment, which is indicative of phosphorylation of the intracellular ITAMs. The FcR has no inherent kinase activity, so why does clustering promote receptor activation? ITAM phosphorylation is controlled by the opposing actions of Src family kinases, which favor activation, and transmembrane phosphatases like CD45 that deactivate the receptor.[1] Prior work has shown that CD45 is excluded from FcR clusters at the phagocytic synapse, and we found that CD45 was also excluded from optoFcR clusters (Figure S1).[36–38] CD45 exclusion can be driven by the extracellular domain, which is too bulky to enter the spatially restricted synapse between a macrophage and its target.[37–39] The CD45 transmembrane domain is also excluded from lipid-ordered domains that are enriched in immune receptors and Src kinases, and the intracellular domain is excluded from clusters of purified receptor intracellular domains on a supported lipid bilayer.[40–42] The optoFcR is myristoylated, so clustering may exclude CD45 due to inclusion of the optoFcR in lipid-ordered domains or clustering of the intracellular domain. In addition, there may be factors other than CD45 exclusion that promote optoFcR phosphorylation and activation, like the geometry of the clustered intracellular FcR domains.

Prior work has shown that a critical threshold of FcR activation is required for macrophages to commit to phagocytosis.[10] FcR signaling that is below this threshold activates the initial steps in the phagocytic signaling pathway, including recruitment of the downstream effector kinase Syk.[10] Whether this low level of activation has any effect on macrophages was not clear. Our data suggest that this low level of activation may have a function in the macrophage, allowing the cell to prepare for future encounters with IgG-bound targets.

In the hour following optoFcR activation, the mobility of native FcRs on the macrophage surface increases. Our working model is that increased FcR mobility increases the formation of receptor clusters that promote initiating and continuing phagocytosis.[21,33] This could enhance macrophage sensitivity by enabling formation of signaling clusters with a lower overall IgG density. Supporting this model, our kinetic analysis shows that short-term priming enhances the same steps in phagocytosis as ligand clustering (Figure 6).[21] FcR mobility is constrained by the actin cytoskeleton and actin-associated transmembrane pickets.[29,31,32,43] Syk kinase activation rearranges the actin cytoskeleton allowing for less constrained FcR diffusion and greater mobility.[31] Because the optoFcR also recruits Syk, changes in the actin cytoskeleton may underlie the change in FcR mobility in our system. Prior studies have correlated FcR or IgG mobility with dramatic impacts on phagocytosis.[29,33] However, our data do not rule out other mechanisms for short-term priming that could synergize with enhanced FcR mobility.

contact with cell), initiation (formation of the phagocytic cup), and completion (cup closure and bead internalization). Below, the percentage of macrophage-bead contacts that progress from one stage to the next.
(D) Representative images of each stage. White box shows area of inset. Scale bar is 10 μm. See also Video S6.
(E) Binding is comparable between primed and unprimed macrophages at 12 h post stimulation.
(F) Percent of bead contacts that initiate phagocytosis is higher in primed macrophages at 12 h after stimulation.
(G) Time from binding to initiation is not changed 12 h post stimulation.
(H) Percent of initiated cups that complete phagocytosis is increased in primed macrophages 12 h post stimulation.
(I) Time from initiation to completion is faster in primed macrophages 12 h after stimulation.
(J) The overall success rate of phagocytosis is increased in primed macrophages.
Each filled data point represents the mean of an independent experiment, denoted by symbol shape, and corresponding outlined data points represent individual bead times. Bars represent the mean ± SEM. *indicates $p < 0.05$, **indicates $p < 0.005$, ***indicates $p < 0.0005$, ****indicates $p < 0.0001$ using an unpaired t test on the means of each replicate.
See also Figure S4, Table S1, and Video S6.

Please cite this article in press as: Bond et al., Prior Fc receptor activation primes macrophages for increased sensitivity to IgG via long-term and short-term mechanisms, Developmental Cell (2024), https://doi.org/10.1016/j.devcel.2024.07.017

CellPress
OPEN ACCESS

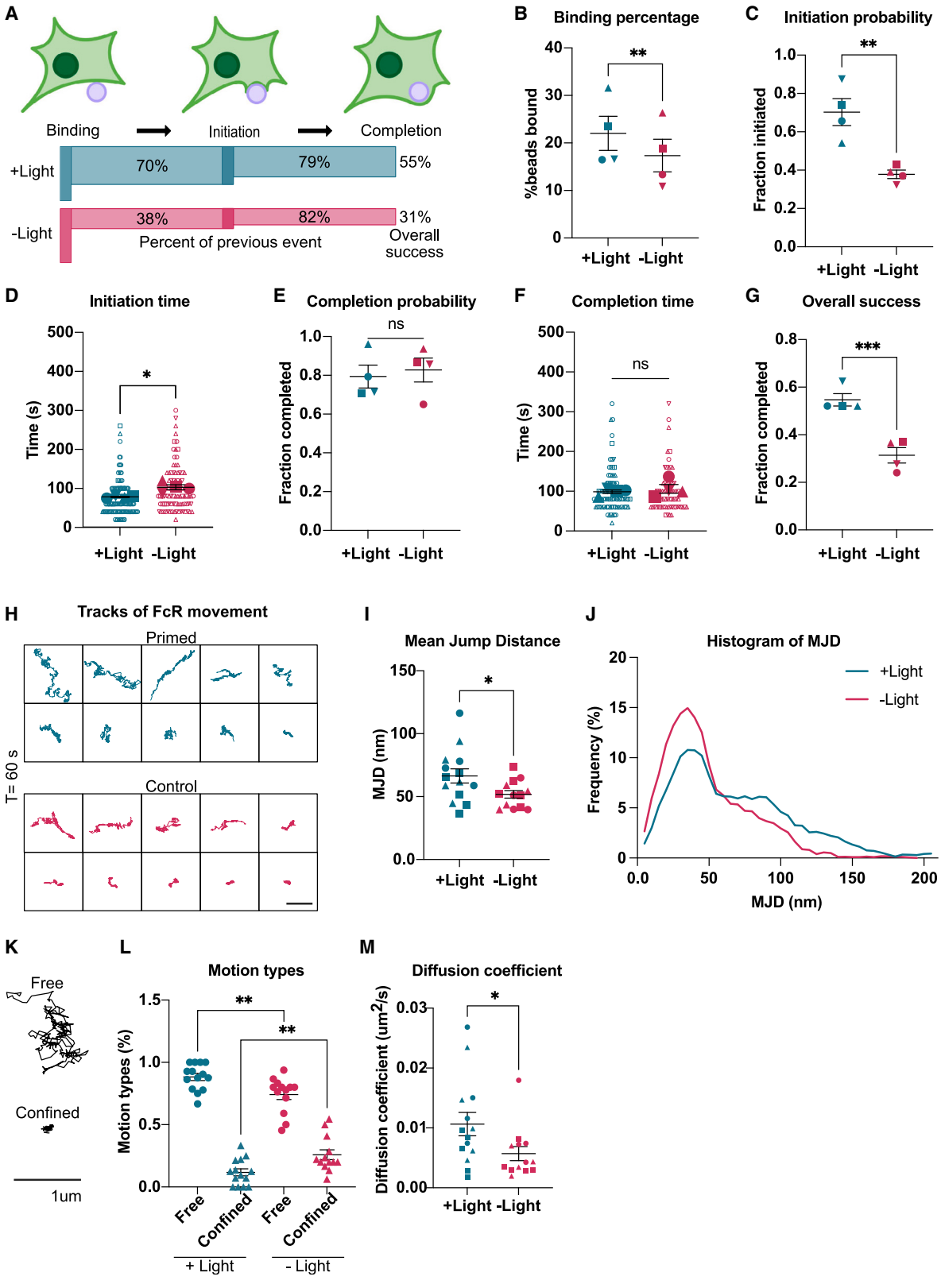

(legend on next page)

Please cite this article in press as: Bond et al., Prior Fc receptor activation primes macrophages for increased sensitivity to IgG via long-term and short-term mechanisms, Developmental Cell (2024), https://doi.org/10.1016/j.devcel.2024.07.017

For example, we found that bead binding was increased in primed macrophages, which could potentially be explained by an increase in FcR mobility, but alternatively could indicate an increase in FcR accessibility.[29]

4 h after FcR activation, the macrophage response to IgG relies on changes in gene expression. We found that these changes in gene expression somewhat correlate with M2 differentiation. Macrophage polarization *in vivo* is known to be more complex than these classic examples, so future studies could determine how exposure to IgG affects the balance of different macrophage subsets. Our kinetics analysis shows that these transcriptional changes drive priming by enhancing multiple stages of phagocytosis, including an increase in the speed of cup closure. This appears to be a different mechanism from short-term priming, which specifically affects the early stages of phagocytosis—bead binding and initiation.

Our data show that lower levels of optoFcR stimulation prime phagocytosis better than high levels. Prior work has shown that low levels of Toll-like receptor (TLR) activation prime macrophages for a rapid and strong response to future stimuli, without activating an inflammatory response alone.[11] Our study suggests this may be true for the FcR pathway as well. The effect of high levels of FcR activation may be different because it is associated with receptor internalization, which can lead to decreased phagocytic capacity.[18] Previous studies have shown that phagocytosing many antibody-coated cancer cells causes macrophage "hypophagia" or reduced phagocytosis. This suggests that the signaling consequences of successful phagocytosis and subthreshold FcR activation may be quite different.

Although the adaptive immune system is traditionally thought of as the source of immunological memory, a growing body of evidence shows that the innate immune system also remembers prior infections and threats. This is often called "trained immunity" and occurs via epigenetic reprogramming of myeloid cells to increase or decrease their transcriptional response to reinfection.[16,44,45] Trained immunity can persist for years if myeloid progenitor cells are affected. Most of the work on trained immunity has focused on a memory of pathogenic molecules or inflammatory cytokines. Our work builds on this, suggesting that FcR activation also elicits a long-term molecular memory driven by Erk-dependent transcriptional changes. Whether this memory persists beyond 72 h will need to be addressed in follow-up *in vivo* studies. In contrast, the short-term priming we describe is distinct from prior descriptions of trained immunity because it does not involve changes in gene expression. We imagine this increased appetite after FcR activation could promote phagocytosis during an infection, when a macrophage is encountering antibody-bound pathogens, while still maintaining a high threshold for activating phagocytosis during homeostasis, when preventing autoimmune disease is a high priority.

The FcR is required for the full efficacy of many cancer immunotherapies, including popular immunotherapies like PD-1 and CTLA-4 blockades.[9,46] Some therapies, like the anti-CD20 antibody rituximab, heavily rely on ADCP as a mechanism for eliminating cancer cells.[4] Interestingly, more frequent low-dose treatments of rituximab are more effective at treating chronic lymphocytic leukemia (CLL) patients than higher-dose treatments.[28] A key reason for this dosing schedule is to mitigate antigen shaving or trogocytosis of target antigen. Enhancing phagocytosis without increasing antigen shaving is important but difficult. Our data show that primed macrophages are better at phagocytosing whole cancer cells but are equally likely to trogocytose. This suggests that the current dosing regimen of frequent, low doses may already benefit from the effects of macrophage priming. Additionally, monocytes expressing chimeric antigen receptors that signal through the FcR intracellular signaling domain are an exciting avenue of cancer research.[47–50] How can we engineer hungrier macrophages to

Figure 6. Short-term priming is caused by an increase in the speed and frequency of initiating phagocytosis, which correlates with an increase in FcR mobility

(A) OptoFcR macrophages received a 15-min light stimulus 1 h before bead addition (primed) and were compared with optoFcR macrophages that did not receive light stimulation (unprimed). Timelapse imaging was used to quantify the kinetics of phagocytosis. Schematic shows each step in phagocytosis: binding (target contact with cell), initiation (formation of the phagocytic cup), and completion (cup closure and bead internalization). Below, the schematic shows percentage of macrophage-bead contacts that progress from one stage to the next.

(B) The percentage of beads bound to primed macrophages is greater in stimulated macrophages.

(C) Percentage of bead contacts that initiate phagocytosis is higher in primed macrophages.

(D) Time from binding to initiation in optoFcR-primed macrophages is decreased compared with unprimed macrophages.

(E) Probability of completing phagocytosis after initiation is comparable in primed and unprimed macrophages.

(F) The speed of cup closure is comparable in primed and unprimed macrophages.

(G) The overall success rate of phagocytosis is higher in primed macrophages compared with unprimed macrophages.

(H) OptoFcR macrophages were primed with a 15-min light stimulus or were not stimulated. 1 h later, we labeled FcRIII (CD16) with a qDot using a FcRIII-specific fab and tracked single FcR molecules for 60 s. All tracks from one representative primed and unprimed image are shown. Scale bar is 1 μm.

(I) Quantification of the per-image mean jump distance (MJD) of all tracks. FcRs from primed macrophages had greater MJD compared with unprimed macrophages.

(J) Histogram of MJD from all acquired tracks from primed and unprimed macrophages. Primed macrophages show an increase in the population of FcRs that have a greater MJD than unprimed macrophages. Histogram was smoothed in prism using a second order polynomial with 6 neighbors on each size.

(K) Examples of "free" and "confined" tracks.

(L) Quantification of motion type analysis shows the proportion of tracks categorized as free (circles) or confined (triangles) for individual images. The percent of tracks defined as free increases in optoFcR-expressing macrophages exposed to light compared with optoFcR macrophages with no light exposure.

(M) Quantification of the per-image mean diffusion coefficients. Tracks from primed macrophages have a higher diffusion coefficient compared with unprimed macrophages.

Each filled data point represents the mean from an independent replicate (B)–(G) or a single image (I)–(M), corresponding outlined data points represent individual bead times (D) and (F). Images were acquired in separate experiments. Bars represent the mean ± SEM. *indicates $p < 0.05$, **indicates $p < 0.005$, ***indicates $p < 0.0005$ using an unpaired t test (B)–(G), (I), and (M) or a one-way ANOVA (L).

See also Figure S5.

Please cite this article in press as: Bond et al., Prior Fc receptor activation primes macrophages for increased sensitivity to IgG via long-term and short-term mechanisms, Developmental Cell (2024), https://doi.org/10.1016/j.devcel.2024.07.017

attack cancer cells? Our studies reveal that macrophage priming could enhance phagocytosis or other anti-cancer signaling pathways in these macrophages.

Limitations of the study

In vivo, there are many specialized macrophage sub-populations. Future studies will need to determine whether IgG primes all of these populations using a similar mechanism or whether there are tissue-specific differences. Future studies should also determine whether therapeutic monoclonal antibodies prime macrophages *in vivo* or in human tissues. The FcR family includes activating and inhibiting receptors. The optoFcR models activating receptors, so future studies will need to address the role of inhibitory FcRs in IgG priming.

STAR★METHODS

Detailed methods are provided in the online version of this paper and include the following:

- KEY RESOURCES TABLE
- RESOURCE AVAILABILITY
  - Lead contact
  - Materials availability
  - Data and code availability
- EXPERIMENTAL MODEL AND STUDY PARTICIPANT DETAILS
  - Bone-marrow derived macrophage cell culture
  - Cell lines
  - Lentivirus production and infection
- METHOD DETAILS
  - Optogenetic stimulation
  - Clustering and colocalization analysis
  - ICAM-1 protein purification
  - Supported lipid bilayer coated beads
  - Bead preparation
  - Phagocytosis assay
  - Inhibitors
  - Bead priming
  - Flow Cytometry
  - Raji eating assay (optoFcR priming)
  - Raji eating assay (Raji priming)
  - Gene expression analysis
  - Receptor labeling and single particle tracking
  - Microscopy
- QUANTIFICATION AND STATISTICAL ANALYSIS

SUPPLEMENTAL INFORMATION

Supplemental information can be found online at https://doi.org/10.1016/j.devcel.2024.07.017.

ACKNOWLEDGMENTS

We thank members of the Morrissey lab for critical feedback on this manuscript. This work was supported by the UCSB Academic Senate, NIGMS (R35GM146935), and the UC Cancer Research Coordinating Committee (C23CR5592) to M.A.M.; the Eunice Kennedy Shriver NICHD (R01HD099517) and the National Human Genome Research Institute (R01HG011013) to S.S.D.; and the Eunice Kennedy Shriver NICHD (R01HD10880301) to M.Z.W. A.B. was supported by the Karl Storz Imaging fellowship. J.E.Q.N. was supported by a supplement to C23CR5592, the EUREKA scholars program, and the MARC scholars program. A.G. was supported by the MARC scholars program. D.J.A. was supported by the NSF CAREER award (CMMI-CAREER-2048043). Schematics were created with BioRender.com. We thank the NRI-MCDB Microscopy Facility at UCSB, especially the director Ben Lopez for providing advice.

AUTHOR CONTRIBUTIONS

Conceptualization, A.B., M.Z.W., and M.A.M.; methodology, A.B., M.Z.W., and M.A.M.; software, K.R., D.J.A., and S.J.R.; validation, A.B.; formal analysis, A.B., S.F., K.R., E.T.S., D.J.A., and S.J.R.; investigation, A.B., S.F., J.E.Q.N., E.T.S., and A.G.; resources, A.B., S.S.D., and M.A.M.; writing – original draft, A.B. and M.A.M.; writing – review and editing, A.B. and M.A.M.; visualization, A.B.; supervision, M.A.M.; funding acquisition, M.A.M., M.Z.W., and S.S.D.

DECLARATION OF INTERESTS

The authors A.B., M.Z.W., and M.A.M. have filed a patent relating to this material.

Received: November 14, 2023
Revised: April 17, 2024
Accepted: July 16, 2024
Published: August 12, 2024

REFERENCES

1. Freeman, S.A., and Grinstein, S. (2014). Phagocytosis: Receptors, signal integration, and the cytoskeleton. Immunol. Rev. *262*, 193–215. https://doi.org/10.1111/imr.12212.
2. Nimmerjahn, F., and Ravetch, J.V. (2008). Fcγ receptors as regulators of immune responses. Nat. Rev. Immunol. *8*, 34–47. https://doi.org/10.1038/nri2206.
3. Gül, N., Babes, L., Siegmund, K., Korthouwer, R., Bögels, M., Braster, R., Vidarsson, G., ten Hagen, T.L.M., Kubes, P., and van Egmond, M. (2014). Macrophages eliminate circulating tumor cells after monoclonal antibody therapy. J. Clin. Invest. *124*, 812–823. https://doi.org/10.1172/JCI66776.
4. Weiskopf, K., and Weissman, I.L. (2015). Macrophages are critical effectors of antibody therapies for cancer. mAbs *7*, 303–310. https://doi.org/10.1080/19420862.2015.1011450.
5. Montalvao, F., Garcia, Z., Celli, S., Breart, B., Deguine, J., Van Rooijen, N.V., and Bousso, P. (2013). The mechanism of anti-CD20–mediated B cell depletion revealed by intravital imaging. J. Clin. Invest. *123*, 5098–5103. https://doi.org/10.1172/JCI70972.
6. Uchida, J., Hamaguchi, Y., Oliver, J.A., Ravetch, J.V., Poe, J.C., Haas, K.M., and Tedder, T.F. (2004). The innate mononuclear phagocyte network depletes B lymphocytes through Fc receptor-dependent mechanisms during anti-CD20 antibody immunotherapy. J. Exp. Med. *199*, 1659–1669. https://doi.org/10.1084/jem.20040119.
7. Watanabe, M., Wallace, P.K., Keler, T., Deo, Y.M., Akewanlop, C., and Hayes, D.F. (1999). Antibody dependent cellular phagocytosis (ADCP) and antibody dependent cellular cytotoxicity (ADCC) of breast cancer cells mediated by bispecific antibody, MDX-210. Breast Cancer Res. Treat. *53*, 199–207. https://doi.org/10.1023/A:1006145507567.
8. Chen, X., Song, X., Li, K., and Zhang, T. (2019). FcγR-Binding Is an Important Functional Attribute for Immune Checkpoint Antibodies in Cancer Immunotherapy. Front. Immunol. *10*, 292. https://doi.org/10.3389/fimmu.2019.00292.
9. Dahan, R., Sega, E., Engelhardt, J., Selby, M., Korman, A.J., and Ravetch, J.V. (2015). FcγRs Modulate the Anti-tumor Activity of Antibodies Targeting the PD-1/PD-L1 Axis. Cancer Cell *28*, 285–295. https://doi.org/10.1016/j.ccell.2015.08.004.
10. Zhang, Y., Hoppe, A.D., and Swanson, J.A. (2010). Coordination of Fc receptor signaling regulates cellular commitment to phagocytosis. Proc. Natl. Acad. Sci. USA *107*, 19332–19337. https://doi.org/10.1073/pnas.1008248107.
11. Gottschalk, R.A., Martins, A.J., Angermann, B.R., Dutta, B., Ng, C.E., Uderhardt, S., Tsang, J.S., Fraser, I.D.C., Meier-Schellersheim, M., and Germain, R.N. (2016). Distinct NF-κB and MAPK Activation Thresholds Uncouple Steady-State Microbe Sensing from Anti-pathogen Inflammatory

Please cite this article in press as: Bond et al., Prior Fc receptor activation primes macrophages for increased sensitivity to IgG via long-term and short-term mechanisms, Developmental Cell (2024), https://doi.org/10.1016/j.devcel.2024.07.017

Responses. Cell Syst. *2*, 378–390. https://doi.org/10.1016/j.cels.2016.04.016.

12. Bettadapur, A., Miller, H.W., and Ralston, K.S. (2020). Biting off what can be chewed: Trogocytosis in health, infection, and disease. Infect. Immun. *88*, e00930-19. https://doi.org/10.1128/IAI.00930-19.

13. Velmurugan, R., Challa, D.K., Ram, S., Ober, R.J., and Ward, E.S. (2016). Macrophage-Mediated Trogocytosis Leads to Death of Antibody-Opsonized Tumor Cells. Mol. Cancer Ther. *15*, 1879–1889. https://doi.org/10.1158/1535-7163.MCT-15-0335.

14. Beum, P.V., Peek, E.M., Lindorfer, M.A., Beurskens, F.J., Engelberts, P.J., Parren, P.W.H.I., van de Winkel, J.G.J., and Taylor, R.P. (2011). Loss of CD20 and bound CD20 antibody from opsonized B cells occurs more rapidly because of trogocytosis mediated by Fc receptor-expressing effector cells than direct internalization by the B cells. J. Immunol. *187*, 3438–3447. https://doi.org/10.4049/JIMMUNOL.1101189.

15. Pham, T., Mero, P., and Booth, J.W. (2011). Dynamics of Macrophage Trogocytosis of Rituximab-Coated B Cells. PLoS One *6*, e14498. https://doi.org/10.1371/journal.pone.0014498.

16. Weavers, H., Evans, I.R., Martin, P., and Wood, W. (2016). Corpse Engulfment Generates a Molecular Memory that Primes the Macrophage Inflammatory Response. Cell *165*, 1658–1671. https://doi.org/10.1016/j.cell.2016.04.049.

17. Sharma, P., Vijaykumar, A., Raghavan, J.V., Rananaware, S.R., Alakesh, A., Bodele, J., Rehman, J.U., Shukla, S., Wagde, V., Nadig, S., et al. (2022). Particle uptake driven phagocytosis in macrophages and neutrophils enhances bacterial clearance. J. Control. Release *343*, 131–141. https://doi.org/10.1016/j.jconrel.2022.01.030.

18. Pinney, J.J., Rivera-Escalera, F., Chu, C.C., Whitehead, H.E., Vandermeid, K.R., Nelson, A.M., Barbeau, M.C., Zent, C.S., and Elliott, M.R. (2020). Macrophage hypophagia as a mechanism of innate immune exhaustion in mAb-induced cell clearance. Blood *136*, 2065–2079. https://doi.org/10.1182/BLOOD.2020005571.

19. Zent, C.S., and Elliott, M.R. (2017). Maxed out macs: physiologic cell clearance as a function of macrophage phagocytic capacity. FEBS J. *284*, 1021–1039. https://doi.org/10.1111/febs.13961.

20. Goodridge, H.S., Underhill, D.M., and Touret, N. (2012). Mechanisms of Fc Receptor and Dectin-1 Activation for Phagocytosis. Traffic *13*, 1062–1071. https://doi.org/10.1111/j.1600-0854.2012.01382.x.

21. Kern, N., Dong, R., Douglas, S.M., Vale, R.D., and Morrissey, M.A. (2021). Tight nanoscale clustering of Fcγ receptors using DNA origami promotes phagocytosis. eLife *10*, e68311. https://doi.org/10.7554/eLife.68311.

22. Sobota, A., Strzelecka-Kiliszek, A., Gładkowska, E., Yoshida, K., Mrozińska, K., and Kwiatkowska, K. (2005). Binding of IgG-Opsonized Particles to FcγR Is an Active Stage of Phagocytosis That Involves Receptor Clustering and Phosphorylation. J. Immunol. *175*, 4450–4457. https://doi.org/10.4049/jimmunol.175.7.4450.

23. Taslimi, A., Vrana, J.D., Chen, D., Borinskaya, S., Mayer, B.J., Kennedy, M.J., and Tucker, C.L. (2014). An optimized optogenetic clustering tool for probing protein interaction and function. Nat. Commun. *5*, 4925. https://doi.org/10.1038/ncomms5925.

24. Springer, T.A., and Dustin, M.L. (2012). Integrin inside-out signaling and the immunological synapse. Curr. Opin. Cell Biol. *24*, 107–115. https://doi.org/10.1016/j.ceb.2011.10.004.

25. Morrissey, M.A., Kern, N., and Vale, R.D. (2020). CD47 Ligation Repositions the Inhibitory Receptor SIRPA to Suppress Integrin Activation and Phagocytosis. Immunity *53*, 290–302.e6. https://doi.org/10.1016/j.immuni.2020.07.008.

26. Vorselen, D., Kamber, R.A., Labitigan, R.L.D., van Loon, A.P., Peterman, E., Delgado, M.K., Lin, S., Rasmussen, J.P., Bassik, M.C., and Theriot, J.A. (2022). Cell surface receptors TREM2, CD14 and integrin αMβ2 drive sinking engulfment in phosphatidylserine-mediated phagocytosis. Preprint at bioRxiv. https://doi.org/10.1101/2022.07.30.502145.

27. Williamson, A.P., and Vale, R.D. (2018). Spatial control of Draper receptor signaling initiates apoptotic cell engulfment. J. Cell Biol. *217*, 3977–3992. https://doi.org/10.1083/jcb.201711175.

28. Williams, M.E., Densmore, J.J., Pawluczkowycz, A.W., Beum, P.V., Kennedy, A.D., Lindorfer, M.A., Hamil, S.H., Eggleton, J.C., and Taylor, R.P. (2006). Thrice-Weekly Low-Dose Rituximab Decreases CD20 Loss via Shaving and Promotes Enhanced Targeting in Chronic Lymphocytic Leukemia1. J. Immunol. *177*, 7435–7443. https://doi.org/10.4049/jimmunol.177.10.7435.

29. Freeman, S.A., Vega, A., Riedl, M., Collins, R.F., Ostrowski, P.P., Woods, E.C., Bertozzi, C.R., Tammi, M.I., Lidke, D.S., Johnson, P., et al. (2018). Transmembrane Pickets Connect Cyto- and Pericellular Skeletons Forming Barriers to Receptor Engagement. Cell *172*, 305–317.e10. https://doi.org/10.1016/j.cell.2017.12.023.

30. Kusumi, A., Fujiwara, T.K., Chadda, R., Xie, M., Tsunoyama, T.A., Kalay, Z., Kasai, R.S., and Suzuki, K.G.N. (2012). Dynamic Organizing Principles of the Plasma Membrane that Regulate Signal Transduction: Commemorating the Fortieth Anniversary of Singer and Nicolson's Fluid-Mosaic Model. Annu. Rev. Cell Dev. Biol. *28*, 215–250. https://doi.org/10.1146/annurev-cellbio-100809-151736.

31. Jaumouillé, V., Farkash, Y., Jaqaman, K., Das, R., Lowell, C.A., and Grinstein, S. (2014). Actin Cytoskeleton Reorganization by Syk Regulates Fcγ Receptor Responsiveness by Increasing Its Lateral Mobility and Clustering. Dev. Cell *29*, 534–546. https://doi.org/10.1016/j.devcel.2014.04.031.

32. Andrews, N.L., Lidke, K.A., Pfeiffer, J.R., Burns, A.R., Wilson, B.S., Oliver, J.M., and Lidke, D.S. (2008). Actin restricts FcepsilonRI diffusion and facilitates antigen-induced receptor immobilization. Nat. Cell Biol. *10*, 955–963. https://doi.org/10.1038/ncb1755.

33. Jo, S., Fischer, B.R., Cronin, N.M., Nurmalasari, N.P.D., Loyd, Y.M., Kerkvliet, J.G., Bailey, E.M., Anderson, R.B., Scott, B.L., and Hoppe, A.D. (2024). Antibody surface mobility amplifies FcγR signaling via Arp2/3 during phagocytosis. Published online February 5, 2024. Biophys. J. *123*. https://doi.org/10.1016/j.bpj.2024.01.036.

34. Duchemin, A.M., Ernst, L.K., and Anderson, C.L. (1994). Clustering of the high affinity Fc receptor for immunoglobulin G (Fc gamma RI) results in phosphorylation of its associated gamma-chain. J. Biol. Chem. *269*, 12111–12117. https://doi.org/10.1016/S0021-9258(17)32688-1.

35. Lin, J., Kurilova, S., Scott, B.L., Bosworth, E., Iverson, B.E., Bailey, E.M., and Hoppe, A.D. (2016). TIRF imaging of Fc gamma receptor microclusters dynamics and signaling on macrophages during frustrated phagocytosis. BMC Immunol. *17*, 5. https://doi.org/10.1186/s12865-016-0143-2.

36. Goodridge, H.S., Reyes, C.N., Becker, C.A., Katsumoto, T.R., Ma, J., Wolf, A.J., Bose, N., Chan, A.S.H., Magee, A.S., Danielson, M.E., et al. (2011). Activation of the innate immune receptor Dectin-1 upon formation of a 'phagocytic synapse'. Nature *472*, 471–475. https://doi.org/10.1038/nature10071.

37. Bakalar, M.H., Joffe, A.M., Schmid, E.M., Son, S., Podolski, M., and Fletcher, D.A. (2018). Size-Dependent Segregation Controls Macrophage Phagocytosis of Antibody-Opsonized Targets. Cell *174*, 131–142.e13. https://doi.org/10.1016/j.cell.2018.05.059.

38. Freeman, S.A., Goyette, J., Furuya, W., Woods, E.C., Bertozzi, C.R., Bergmeier, W., Hinz, B., van der Merwe, P.A., Das, R., and Grinstein, S. (2016). Integrins Form an Expanding Diffusional Barrier that Coordinates Phagocytosis. Cell *164*, 128–140. https://doi.org/10.1016/j.cell.2015.11.048.

39. James, J.R., and Vale, R.D. (2012). Biophysical mechanism of T-cell receptor triggering in a reconstituted system. Nature *487*, 64–69. https://doi.org/10.1038/nature11220.

40. Stone, M.B., Shelby, S.A., Núñez, M.F., Wisser, K., and Veatch, S.L. (2017). Protein sorting by lipid phase-like domains supports emergent signaling function in b lymphocyte plasma membranes. eLife *6*, 1–33. https://doi.org/10.7554/eLife.19891.

Please cite this article in press as: Bond et al., Prior Fc receptor activation primes macrophages for increased sensitivity to IgG via long-term and short-term mechanisms, Developmental Cell (2024), https://doi.org/10.1016/j.devcel.2024.07.017

41. Su, X., Ditlev, J.A., Rosen, M.K., and Vale, R.D. (2017). Reconstitution of TCR signaling using supported lipid bilayers. Methods Mol. Biol. *1584*, 65–76. https://doi.org/10.1007/978-1-4939-6881-7_5.

42. Shelby, S.A., and Veatch, S.L. (2023). The Membrane Phase Transition Gives Rise to Responsive Plasma Membrane Structure and Function. Cold Spring Harb. Perspect. Biol. *15*, a041395. https://doi.org/10.1101/cshperspect.a041395.

43. Jaumouillé, V., and Grinstein, S. (2011). Receptor mobility, the cytoskeleton, and particle binding during phagocytosis. Curr. Opin. Cell Biol. *23*, 22–29. https://doi.org/10.1016/j.ceb.2010.10.006.

44. Netea, M.G., Domínguez-Andrés, J., Barreiro, L.B., Chavakis, T., Divangahi, M., Fuchs, E., Joosten, L.A.B., van der Meer, J.W.M., Mhlanga, M.M., Mulder, W.J.M., et al. (2020). Defining trained immunity and its role in health and disease. Nat. Rev. Immunol. *20*, 375–388. https://doi.org/10.1038/s41577-020-0285-6.

45. Tehrani, S.S.H., Kogan, A., Mikulski, P., and Jansen, L.E.T. (2023). Remembering foods and foes: emerging principles of transcriptional memory. Published online August 10, 2023. Cell Death Differ. https://doi.org/10.1038/s41418-023-01200-6.

46. Simpson, T.R., Li, F., Montalvo-Ortiz, W., Sepulveda, M.A., Bergerhoff, K., Arce, F., Roddie, C., Henry, J.Y., Yagita, H., Wolchok, J.D., et al. (2013). Fc-dependent depletion of tumor-infiltrating regulatory T cells co-defines the efficacy of anti-CTLA-4 therapy against melanoma. J. Exp. Med. *210*, 1695–1710. https://doi.org/10.1084/jem.20130579.

47. Morrissey, M.A., Williamson, A.P., Steinbach, A.M., Roberts, E.W., Kern, N., Headley, M.B., and Vale, R.D. (2018). Chimeric antigen receptors that trigger phagocytosis. eLife *7*, e36688. https://doi.org/10.7554/eLife.36688.

48. Klichinsky, M., Ruella, M., Shestova, O., Lu, X.M., Best, A., Zeeman, M., Schmierer, M., Gabrusiewicz, K., Anderson, N.R., Petty, N.E., et al. (2020). Human chimeric antigen receptor macrophages for cancer immunotherapy. Nat. Biotechnol. *38*, 947–953. https://doi.org/10.1038/s41587-020-0462-y.

49. Sloas, C., Gill, S., and Klichinsky, M. (2021). Engineered CAR-Macrophages as Adoptive Immunotherapies for Solid Tumors. Front. Immunol. *12*, 783305. https://doi.org/10.3389/fimmu.2021.783305.

50. Wang, S., Yang, Y., Ma, P., Zha, Y., Zhang, J., Lei, A., and Li, N. (2022). CAR-macrophage: An extensive immune enhancer to fight cancer. EBioMedicine *76*, 103873. https://doi.org/10.1016/j.ebiom.2022.103873.

51. O'Donoghue, G.P., Pielak, R.M., Smoligovets, A.A., Lin, J.J., and Groves, J.T. (2013). Direct single molecule measurement of TCR triggering by agonist pMHC in living primary T cells. eLife *2*, e00778. https://doi.org/10.7554/eLife.00778.

52. Ershov, D., Phan, M.-S., Pylvänäinen, J.W., Rigaud, S.U., Le Blanc, L., Charles-Orszag, A., Conway, J.R.W., Laine, R.F., Roy, N.H., Bonazzi, D., et al. (2022). TrackMate 7: integrating state-of-the-art segmentation algorithms into tracking pipelines. Nat. Methods *19*, 829–832. https://doi.org/10.1038/s41592-022-01507-1.

53. Tinevez, J.-Y., Perry, N., Schindelin, J., Hoopes, G.M., Reynolds, G.D., Laplantine, E., Bednarek, S.Y., Shorte, S.L., and Eliceiri, K.W. (2017). TrackMate: An open and extensible platform for single-particle tracking. Methods *115*, 80–90. https://doi.org/10.1016/j.ymeth.2016.09.016.

54. Bolte, S., and Cordelières, F.P. (2006). A guided tour into subcellular colocalization analysis in light microscopy. J. Microsc. *224*, 213–232. https://doi.org/10.1111/j.1365-2818.2006.01706.x.

55. Atkins, D.J., Rosas, J.M., Månsson, L.K., Shahverdi, N., Dey, S.S., and Pitenis, A.A. (2024). Survival-Associated Cellular Response Maintained in Pancreatic Ductal Adenocarcinoma (PDAC) Switched Between Soft and Stiff 3D Microgel Culture. ACS Biomater. Sci. Eng. *10*, 2177–2187. https://doi.org/10.1021/acsbiomaterials.3c01079.

56. Höhener, T.C., Landolt, A.E., Dessauges, C., Hinderling, L., Gagliardi, P.A., and Pertz, O. (2022). LITOS: a versatile LED illumination tool for optogenetic stimulation. Sci. Rep. *12*, 13139. https://doi.org/10.1038/s41598-022-17312-x.

57. Weischenfeldt, J., and Porse, B. (2008). Bone Marrow-Derived Macrophages (BMM): Isolation and Applications. CSH Protoc. *2008*, pdb.prot5080. https://doi.org/10.1101/pdb.prot5080.

58. Stewart, S.A., Dykxhoorn, D.M., Palliser, D., Mizuno, H., Yu, E.Y., An, D.S., Sabatini, D.M., Chen, I.S.Y., Hahn, W.C., Sharp, P.A., et al. (2003). Lentivirus-delivered stable gene silencing by RNAi in primary cells. RNA *9*, 493–501. https://doi.org/10.1261/rna.2192803.

59. Hui, E., and Vale, R.D. (2014). In vitro membrane reconstitution of the T-cell receptor proximal signaling network. Nat. Struct. Mol. Biol. *21*, 133–142. https://doi.org/10.1038/nsmb.2762.

60. Hashimshony, T., Senderovich, N., Avital, G., Klochendler, A., de Leeuw, Y., Anavy, L., Gennert, D., Li, S., Livak, K.J., Rozenblatt-Rosen, O., et al. (2016). CEL-Seq2: sensitive highly-multiplexed single-cell RNA-Seq. Genome Biol. *17*, 77. https://doi.org/10.1186/s13059-016-0938-8.

61. Church, D.M., Schneider, V.A., Graves, T., Auger, K., Cunningham, F., Bouk, N., Chen, H.-C., Agarwala, R., McLaren, W.M., Ritchie, G.R.S., et al. (2011). Modernizing Reference Genome Assemblies. PLoS Biol. *9*, e1001091. https://doi.org/10.1371/journal.pbio.1001091.

62. Love, M.I., Huber, W., and Anders, S. (2014). Moderated estimation of fold change and dispersion for RNA-seq data with DESeq2. Genome Biol. *15*, 550. https://doi.org/10.1186/s13059-014-0550-8.

63. Stephens, M., Carbonetto, P., Dai, C., Gerard, D., Lu, M., Sun, L., Willwerscheid, J., Xiao, N., and Zeng, M. (2023). ashr: Methods for Adaptive Shrinkage, using Empirical Bayes. Version 2.2-63. https://cran.r-project.org/web/packages/ashr/index.html.

64. Ritchie, M.E., Phipson, B., Wu, D., Hu, Y., Law, C.W., Shi, W., and Smyth, G.K. (2015). limma powers differential expression analyses for RNA-sequencing and microarray studies. Nucleic Acids Res. *43*, e47. https://doi.org/10.1093/nar/gkv007.

65. Gu, Z., Eils, R., and Schlesner, M. (2016). Complex heatmaps reveal patterns and correlations in multidimensional genomic data. Bioinformatics *32*, 2847–2849. https://doi.org/10.1093/bioinformatics/btw313.

66. Ferrari, R., Manfroi, A.J., and Young, W.R. (2001). Strongly and weakly self-similar diffusion. Phys. D Nonlinear Phenom. *154*, 111–137. https://doi.org/10.1016/S0167-2789(01)00234-2.

67. Ewers, H., Smith, A.E., Sbalzarini, I.F., Lilie, H., Koumoutsakos, P., and Helenius, A. (2005). Single-particle tracking of murine polyoma virus-like particles on live cells and artificial membranes. Proc. Natl. Acad. Sci. USA *102*, 15110–15115. https://doi.org/10.1073/pnas.0504407102.

68. Jaqaman, K., Kuwata, H., Touret, N., Collins, R., Trimble, W.S., Danuser, G., and Grinstein, S. (2011). Cytoskeletal control of CD36 diffusion promotes its receptor and signaling function. Cell *146*, 593–606. https://doi.org/10.1016/j.cell.2011.06.049.

69. Sbalzarini, I.F., and Koumoutsakos, P. (2005). Feature point tracking and trajectory analysis for video imaging in cell biology. J. Struct. Biol. *151*, 182–195. https://doi.org/10.1016/j.jsb.2005.06.002.

Please cite this article in press as: Bond et al., Prior Fc receptor activation primes macrophages for increased sensitivity to IgG via long-term and short-term mechanisms, Developmental Cell (2024), https://doi.org/10.1016/j.devcel.2024.07.017

STAR★METHODS

KEY RESOURCES TABLE

REAGENT or RESOURCE	SOURCE	IDENTIFIER
Antibodies		
AlexaFlour647 anti-biotin IgG	Jackson ImmunoResearch Laboratories	Cat# 200-602-211; RRID: AB_2339046
Anti-CD20	InvivoGen	Cat# hcd20-mab10; RRID: AB_11124933
Mouse Anti-CD16/32	Cell signaling	Cat# 88280
Anti-Rat IgG biotin conjugate	Invitrogen	Cat# 13-4813-85
Anti-CD45	Cell Signaling	Cat# 70257T
Anti-Rabbit 488	Cell Signaling	Cat# 4412S
Anti-CD44 Superbright 600	Invitrogen	Cat# 63-044-82
Anti-CD64 PerCP-eFuor710	Invitrogen	Cat# 46-0641-80
Anti-CD16-2 FITC	Invitrogen	Cat# MA-28253
Anti-CD32b APC	Invitrogen	Cat# 17-0321-80
Anti-CD16/32 PE	Biolegend	Cat# 101307; RRID: AB_312806
Anti-SIRPa APC/Cy7	Biolegend	Cat# 144018; RRID: AB_2629558
Superbright 600 isotype control	Invitrogen	Cat# 634031-82
PerCP-eFuor710 isotype control	Invitrogen	Cat# 46-4714-80
FITC isotype control	Biolegend	Cat# 402307; RRID: AB_3097095
APC isotype control	Invitrogen	Cat# 17-4724-81
PE isotype control	Invitrogen	Cat# 12-4321-80
APC/Cy7 isotype control	Biolegend	Cat# 400422; RRID: AB_830905
Chemicals, peptides, and recombinant proteins		
POPC	Avanti	Cat# 850457
Biotinyl cap PE	Avanti	Cat# 870273
PEG5000-PE	Avanti	Cat# 880230
Atto390-DOPE	ATTO-TEC GmbH	Cat# AD 390-161
Atto647-DOPE	ATTO-TEC GmbH	Cat# AD 647-161
Ni2+-DGS-NTA	Avanti	Cat# 790404
DOPS	Avanti	Cat# 840035
CellTrace Far Red	ThermoFisher	Cat# C34572
CellTrace CSFE	ThermoFisher	Cat# C34570
Qdot 655	ThermoFisher	Cat# Q10123MP
Casein	Sigma	Cat# C5890
PD0325901 - ERK inhibitor	Sigma	Cat# PZ0162
Actinomycin D	Cell signaling	Cat# 15021s
Cycloheximide	Cell signaling	Cat# 2112s
dNTPs	New England Biolabs	Cat# N0447l
RNase OUT	ThermoFisher	Cat# 10777019
Superscript II Reverse Transcriptase	Invitrogen	Cat# 1864014
E. coli DNA Polymerase I	Invitrogen	Cat# 18010025
RNase H	ThermoFisher	Cat# EN0202
DNA magnetic beads	AMPure	Cat# A63882
MEGAscript T7	Invitrogen	Cat# A57622
ExoSAP IT PCR reagent	Invitrogen	Cat# 78200.200.UL
LPS	Sigma	Cat# L4516
IFN-y	Sino Biological	Cat# 50709-MNAH
IL-4	Sino Biological	Cat# 51084-MNAE

(*Continued on next page*)

Please cite this article in press as: Bond et al., Prior Fc receptor activation primes macrophages for increased sensitivity to IgG via long-term and short-term mechanisms, Developmental Cell (2024), https://doi.org/10.1016/j.devcel.2024.07.017

CellPress
OPEN ACCESS

Continued

REAGENT or RESOURCE	SOURCE	IDENTIFIER
Critical commercial assays		
Pierce Fab Preparation Kit	ThermoFisher	Cat# 44985
PureLink RNA mini kit	Invitrogen	Cat# 12183018A
Experimental models: Cell lines		
Human: HEK239T	ATCC	Cat# ATCC CRL-3216
Mouse: RAW264.7	ATCC	Cat# ATCC TIB-71; RRID:CVCL_0493
Mouse: L929	ATCC	Cat# ATCC CLL1; RRID:CVCL_0462
Sf9	ThermoFisher	Cat# 11496015
Experimental models: Organisms/strains		
Mouse: C57BL/6	The Jackson Laboratory	Cat# 000664
Recombinant DNA		
pHR-optoFcR	This paper	In pHR vector. Myristolization sequence: MGSSKSKPKDPSQR; cytoplasmic domain (aa 45–86) of the Fc γ-chain UniProtKB - P20491 (FCERG_MOUSE); linker: STSG; fluorophore: mScarlet; linker: SDPGSGS; Cry2-olig (aa 1-498) of CRY2_ARATH UnitprotKB – Q96524 with E490G mutation followed by: ARDPP (as described in Taslimi et al.[23])
pHR-Syk NeonGreen NK83	Kern et al.[21]	Addgene plasmid # 176610; http://n2t.net/addgene:176610; RRID:Addgene_176610
pHR mCherry-caax	Morrissey et al.[47]	mCherry fused to membrane targeting sequence from KRAB (amino acids LEKMSKDGKKKKKKSKTKCVIM)
pMD2.G	pMD2.G was a gift from Didier Trono, Swiss Federal Institute of Technology Lausanne	Addgene plasmid # 12259; http://n2t.net/addgene:12259; RRID:Addgene_12259
pCMV-dR8.2	pCMV-dR8.2 dvpr was a gift from Bob Weinberg, Whitehead Institute for Biomedical Research	Addgene plasmid # 8455; http://n2t.net/addgene:8455; RRID:Addgene_8455
ICAM-tagBFP-His10	O'Donoghue et al.[51]	N/A
Software and algorithms		
ImageJ -Fiji	NIH	RRID:SCR_002285; https://fiji.sc/
Affinity Designer	Serif	RRID:SCR_016952
Prism	Graphpad	RRID:SCR_002798
TrackMate	Ershov et al.[52]; Tinevez et al.[53]	N/A
Moment Scaling Spectrum analysis	This paper	https://github.com/MZW-Lab/Trajectory_Analysis_optoFcR/tree/main; Github: https://doi.org/10.5281/zenodo.12701581
Blind-Analysis-Tools-1.0	Github	https://github.com/ahtsaJ/Blind-Analysis-Tools
JaCoP	Bolte and Cordelières[54]	N/A
FlowJo 10	FlowJo	RRID:SCR_008520
RNAseq analysis	Atkins et al.[55]	N/A
Other		
5 um silica beads	Bangs Labs	Cat# SS05003
MatriPlate	Brooks	Cat# MGB09-1-2-LG-L
LITOS stimulation plate	Höhener et al.[56]	N/A
Alexa Fluor 647 MESF calibration beads	Bangs Labs	Cat# 647
RNAseq data	This paper	DRYAD: https://doi.org/10.5061/dryad.hx3ffbgp1

Please cite this article in press as: Bond et al., Prior Fc receptor activation primes macrophages for increased sensitivity to IgG via long-term and short-term mechanisms, Developmental Cell (2024), https://doi.org/10.1016/j.devcel.2024.07.017

RESOURCE AVAILABILITY

Lead contact

Further information and requests for resources and reagents should be directed to and will be fulfilled by the lead contact, Meghan Morrissey (morrissey@ucsb.edu).

Materials availability

Plasmids generated in this study have been deposited to Addgene or can be obtained from the lead contact.

Data and code availability

- RNA-seq data have been deposited at Dryad and are publicly available as of the date of publication. DOIs are listed in the key resources table. Complete imaging datasets are available from the lead contact upon request.
- All original code has been deposited on GitHub and is publicly available as of the date of publication. DOIs are listed in the key resources table.
- Any additional information required to reanalyze the data reported in this paper is available from the lead contact upon request.

EXPERIMENTAL MODEL AND STUDY PARTICIPANT DETAILS

Bone-marrow derived macrophage cell culture

Six- to ten-week-old male and female C57BL/6 mice were sacrificed by CO2 inhalation. Hips and femurs were dissected and bone marrow was harvested as described in Weischenfeldt and Porse.[57] Macrophage progenitors were differentiated for seven days in RPMI-1640, 10% FBS, 1% PSG supplemented with 20% L929- conditioned media at 37°C. Macrophage differentiation was confirmed by flow cytometry identifying CD11b and F4/80 double positive cells. Differentiated BMDMs were used for experiments from days 7 to 11.

Cell lines

HEK293T cells (ATCC CRL-3216) were obtained from ATCC and were cultured in DMEM, 10% FBS, 1% PSG media at 37°C. RAW264.7 (ATCC TIB-71) cells were obtained from ATCC and were cultured in DMEM, 10% FBS, 1% PSG, 1nM sodium pyruvate.

Lentivirus production and infection

All constructs were expressed in BMDMs using lentiviral infection. Lentivirus was produced in HEK293T cells transfected with pMD2.G (Gift from Didier Trono, Addgene plasmid # 12259 containing the VSV-G envelope protein), pCMV-dR8.2[58] (Gift from Bob Weinberg, Addgene plasmid #8455), and a lentiviral backbone vector containing the construct of interest using lipofectamine LTX (Invitrogen, Cat# 15338–100). The media was harvested 72 h post-transfection, filtered through a 0.45 μm filter (Millapore, Cat# SLHVM33RS) and concentrated using LentiX (Takara Biosciences, Cat# 631232). Concentrated lentivirus was added to cells on day 2 of differentiation. Cells were analyzed between days 7-11.

METHOD DETAILS

Optogenetic stimulation

Cells receiving low intensity light (5 uW/cm^2) and medium intensity light (190 uW/cm^2) were stimulated using a LITOS LED illumination plate[56] for 15 min. Cells receiving high intensity light were stimulated using the 488 laser at 75% laser power on a spinning disc confocal microscope for 1 s at 20 s intervals for a total of 15 m (1,389 uW/cm^2). Intensity was determined using a slide power meter set to measure 450 nm light. Light used to prime cells was low intensity (5 uW/cm^2) unless otherwise indicated.

Clustering and colocalization analysis

Validating optoFcR clustering and Syk colocalization

50,000 BMDMs expressing the optoFcR were plated in one well of a 96-well glass bottom MatriPlate (Brooks, Cat# MGB096-1-2-LG-L) between 12 and 24 h prior to the experiment. Cells were then continuously imaged with high intensity light stimulation for 30 min and then imaged for another 60 min without light stimulation.

To measure optoFcR and Syk colocalization, 50,000 RAW264.7 macrophages virally infected with both the optoFcR and Syk-NeonGreen (Addgene, Plasmid# 176610) were plated in one well of a 96-well glass bottom MatriPlate (Brooks, Cat# MGB096-1-2-LG-L) between 12 and 24 h prior to the experiment. Cells were then continuously imaged with high intensity light stimulation for 30 min. Colocalization was determined by selecting an ROI at the cell membrane, and measuring the Pearson's correlation coefficient at the first and last timepoints using the JaCoP plugin in ImageJ.[54]

OptoFcR cluster characterization of CD45 colocalization

50,000 BMDMs expressing the optoFcR were plated in one well of a 96-well glass bottom MatriPlate (Brooks, Cat# MGB096-1-2-LG-L) between 12 and 24 h prior to the experiment. Cells were then stimulated with low, medium, or high light intensity for 15 min

Please cite this article in press as: Bond et al., Prior Fc receptor activation primes macrophages for increased sensitivity to IgG via long-term and short-term mechanisms, Developmental Cell (2024), https://doi.org/10.1016/j.devcel.2024.07.017

and immediately fixed with 4% PFA. Cells were then imaged with TIRF microscopy. The average number and area of optoFcR clusters was determined using ImageJ with manual selection of clusters.

To visualize CD45, cells were plated and stimulated as above. After fixing, cells were washed in PBS and blocked in PBS + 0.5% BSA for 1 hour. Cells were then incubated in CD45 primary antibody (Cell Signaling, Cat# 70257T) overnight at 4 degrees. Cells were then washed and incubated in anti-rabbit secondary antibody (Cell Signaling, Cat# 4412S) for 2 hours. Cells were imaged with TIRF microscopy and colocalization was determined by a Pearson's correlation coefficient using the JaCoP plugin in ImageJ.[54] ROIs were selected across an entire cell membrane.

ICAM-1 protein purification

ICAM-tagBFP-His_{10}[51] was expressed in SF9 or HiFive cells using the Bac-to-Bac baculovirus system as described previously.[59] Insect cell media containing secreted proteins was harvested 72 h after infection with baculovirus. His10 proteins were purified by using Ni-NTA agarose (QIAGEN, Cat# 30230), followed by size exclusion chromatography using a Superdex 200 10/300 GL column (GE Healthcare, Cat# 17517501). The purification buffer was 150 mM NaCl, 50 mM HEPES pH 7.4, 5% glycerol, 2 mM TCEP.

Supported lipid bilayer coated beads

SUV preparation

For IgG conjugated beads the following chloroform-suspended lipids were mixed and desiccated overnight to remove chloroform: 98.8% POPC (Avanti, Cat# 850457), 1% biotinyl cap PE (Avanti, Cat# 870273), 0.1% PEG5000-PE (Avanti, Cat# 880230, and 0.1% atto390-DOPE (ATTO-TEC GmbH, Cat# AD 390–161) or 0.1% atto647-DOPE (ATTO-TEC GmbH, Cat# AD 647–161). The lipid sheets were resuspended in PBS, pH7.2 (GIBCO, Cat# 20012050) at 10 mM concentration and stored under inert nitrogen gas.

For ICAM-1 conjugated beads, the following chloroform-suspended lipids were mixed and desiccated overnight to remove chloroform: 97.8% POPC (Avanti, Cat# 850457), 2% DGS-NTA (Avanti, Cat# 790404), 0.1% PEG5000-PE (Avanti, Cat# 880230, and 0.1% atto390-DOPE (ATTO-TEC GmbH, Cat# AD 390–161). The lipid sheets were resuspended in PBS, pH7.2 (GIBCO, Cat# 20012050) and stored under inert gas.

For PS beads the following chloroform-suspended lipids were mixed and desiccated overnight to remove chloroform: 89.8% POPC (Avanti, Cat# 850457), 10% DOPS (Avanti, Cat# 840035), 0.1% PEG5000-PE (Avanti, Cat# 880230, and 0.1% atto390-DOPE (ATTO-TEC GmbH, Cat# AD 390–161). The lipid sheets were resuspended in PBS, pH7.2 (GIBCO, Cat# 20012050) and stored under inert gas.

For all SUVs, the lipids were broken into small unilamellar vesicles via several rounds of freeze-thaws. The lipids were then stored at -80°C under argon. To remove aggregated lipids, the solution was diluted to 2 mM and filtered through a 0.22 uM filter (Millapore, Cat# SLLG013SL) immediately prior to use.

Bead preparation

Silica beads with a 4.89 μm diameter (10% solids, Bangs Labs, Cat# SS05003, Lot # 13427) were washed several times with PBS, mixed with 1mM SUVs in PBS and incubated at room temperature for 30 min with end-over-end mixing to allow for bilayer formation. Beads were then washed with PBS to remove excess SUVs and incubated in 0.2% casein (Sigma, Cat# C5890) in PBS for 15 min before protein coupling (IgG and ICAM-1 beads). For IgG conjugated beads, anti-biotin AlexaFluor647-IgG (Jackson ImmunoResearch Laboratories Cat# 200-602-211, Lot# 156182) was added at 1 nM (final density approx. 10-18 IgG molecules/um^2) to a 10x dilution of beads (1% solids), unless otherwise indicated. For ICAM-1 conjugated beads, ICAM-1 was added at 10nM. Proteins were coupled to the bilayer for 30 min at room temperature with end-over-end mixing.

The number of IgG molecules per bead was determined by generating a standard curve using Quantum Alexa Fluor 647 MESF calibration beads (Bangs Labs, Cat# 647) to determine the number of fluorescent molecules per bead. IgG from Jackson Immunoresearch labs is labeled with an average of 3.5-5.5 fluorescent molecules per IgG.

Phagocytosis assay

50,000 BMDMs were plated in one well of a 96-well glass bottom MatriPlate (Brooks, Cat# MGB096-1-2-LG-L) between 12 and 24 h prior to the experiment. ~8×10^5 beads were added to wells and engulfment was allowed to proceed for 15 min. The cells were imaged using spinning disc microscopy (40 × 0.95 NA Plan Apo air). Internalized particles were identified by their fluorescent supported lipid bilayer, and counted in ImageJ by a blinded analyzer using Blind-Analysis-Tools-1.0 ImageJ plug in.

Inhibitors

For transcription and translation inhibited priming, 10 nM actinomycin D (Cell signaling, Cat# 15021s) or 10 ug/ml cycloheximide (Cell signaling, Cat# 2112s) were added to cells 7 hours prior to the start of the experiment. For Erk inhibited priming, 0.5 uM PD0325901 (Sigma, Cat# PZ0162) was added to cells 16 hours prior to the start of the experiment.

Bead priming

50,000 BMDMs were plated in 1 well of a 96-well glass bottom plate 12-24 hours prior to the start of the experiment. A priming dose of ~8×10^5 atto390 beads conjugated to either 1 nM or 0 nM IgG were added to the wells for 15 min. Any unengulfed beads were washed out 5x with media, then checked with a dissecting microscope to confirm the majority of unengulfed beads had been

Please cite this article in press as: Bond et al., Prior Fc receptor activation primes macrophages for increased sensitivity to IgG via long-term and short-term mechanisms, Developmental Cell (2024), https://doi.org/10.1016/j.devcel.2024.07.017

removed. Then the cells were allowed to recover for 1 hour. ~8 × 10^5 atto647 beads prepared with the indicated IgG concentrations were then added to the wells and engulfment was allowed to proceed for 15 min in a 37 degree incubator. Cells were dyed with CellTrace CSFE (Thermo, Cat# C34570) imaged and the number of atto647 beads engulfed per cell were counted.

Flow Cytometry

200,000 BMDMs were plated in 1 well of a 12 well glass bottom plate (CellVis, Cat# P12-1.5H-N) 24 hours prior to the start of the experiment and stimulated with low, medium, or high intensity light at 1 or 12 hours prior to the start of the experiment. BMDMs were lifted and then washed in PBS before being resuspended in PBS + 0.5% BSA with the following antibodies for 30 min: CD44 Superbright 600 (Invitrogen, Cat# 63-044-82), Superbright 600 isotype control (Invitrogen, Cat# 634031-82), CD64 PerCP-eFluor 710 (Invitrogen, Cat# 46-0641-80), PerCP-eFluor 710 isotype control (Invitrogen, Cat# 46-4714-80), CD16-2 FITC (Invitrogen, Cat# MA-28253), FITC isotype control (Biolegend, Cat# 402307), CD32b APC (Invitrogen, Cat# 17-0321-80), APC isotype control (Invitrogen, Cat# 17-4724-81), CD16/32 PE (Biolegend, Cat# 101307), PE isotype control (Invitrogen, Cat# 12-4321-80), SIRPa APC/Cy7 (Biolegend, Cat# 144018), APC/Cy7 isotype control (Biolegend, Cat# 400422). Cells were then washed in PBS and analyzed using an Attune NxT (invitrogen). Analysis was completed in FlowJo to assess the median fluorescence intensity of each sample. Compensation was performed using single stain and isotype controls.

Raji eating assay (optoFcR priming)

40,000 BMDMs were plated in 1 well of a 96-well glass bottom plate 24 hours prior to the experiment and stimulated with low intensity LITOS illumination 12 hours prior to the experiment. Raji cells were dyed with CellTrace Far Red (Thermo, Cat# C34572), incubated with a human-mouse hybrid aCD20 (InvivoGen, Cat# hcd20-mab10, 5 ng/ml), added to wells at 40,000 cells per well, and imaged immediately. 25 positions per well were automatically selected and imaged every 3 min for 10 hours. Unless otherwise noted, 100 macrophages were randomly selected and scored by a blind analyzer. Phagocytic macrophages were characterized as BMDMs that engulfed 1 or more whole Raji cell targets. Trogocytic macrophages were characterized as BMDMs that engulfed portions of Raji targets. The number of Raji cells engulfed per 100 macrophages was also counted.

Raji eating assay (Raji priming)

40,000 BMDMs were plated in 1 well of a 96-well glass bottom plate 48 hours prior to the experiment. BMDMs were co-incubated with either control media, Raji cells that were previously incubated with a human-mouse hybrid aCD20 (InvivoGen, Cat# hcd20-mab10, 5 ng/ml), or with unopsonized Raji cells. Plates were spun for 5 min at 300xg to ensure Raji cells reached the BMDMs. Following the spin, priming occurred for 15 min before the remaining Raji cells were thoroughly washed out (~15x). 24 hours after the initial stimulus, Raji cells for the secondary stimulus were dyed with CellTrace Far Red (Thermo, Cat# C34572), incubated with a human-mouse hybrid aCD20 (InvivoGen, Cat# hcd20-mab10, 5 ng/ml), added to wells at 40,000 cells per well, and imaged immediately. 25 positions per well were automatically selected and imaged every 3 min for 10 hours. Unless otherwise noted, 100 macrophages were randomly selected and scored by a blind analyzer. Phagocytic macrophages were characterized as BMDMs that engulfed 1 or more whole Raji cell targets. Trogocytic macrophages were characterized as BMDMs that engulfed portions of Raji targets. The number of Raji cells engulfed per 100 macrophages was also counted.

Gene expression analysis

Macrophage polarization and stimulation

500,000 BMDMs were plated in 1 well of a 6 well glass bottom plate (CellVis, Cat# P06-1.5H-N) 24 hours prior to the start of the stimulation. For M1 polarized cells, 100 ng/ml LPS (Sigma, Cat# L4516) and 50ng/ml IFN-ɣ (Sino Biological, Cat# 50709-MNAH) were added to the cells for 24 hours. For M2 polarized cells, 20 ng/ml IL-4 (Sino Biological, Cat# 51084-MNAE) was added to the cells for 24 hours. The BMDMs were then collected for RNA extraction. Optogenetic stimulation was performed as previously described in these methods with low intensity light for 15 min and cells were collected for RNA extraction 12 hours after stimulation.

RNA Extraction

Total RNA was extracted using PureLink RNA mini kit (Invitrogen, Cat#12183018A) according to the manufacturer's protocol.

RNAseq

Bulk mRNA sequencing using the CEL-Seq2 technique was performed on 10 ng of total RNA per sample according to previously established protocol.[60] Briefly, mRNA fragments were randomly primed and reverse transcribed using dNTPs (New England Biolabs, Cat# N0447l), 0.1 M DTT, RNase OUT (ThermoFisher, Cat# 10777019) and Superscript II Reverse Transcriptase (Invitrogen, Cat# 18064014). Then, cDNA strands were synthesized using dNTPs (New England Biolabs, Cat# N0447l), E. coli DNA Polymerase I (Invitrogen, Cat# 18010025), First Strand Buffer (from Invitrogen Superscript II Reverse Transcriptase, Cat# 18064014), and RNase H (Thermo Scientific, Cat# EN0202). DNA magnetic beads (AMPure, Cat# A63882) were used to purify and size DNA fragments before undergoing in vitro transcription to linearly amplify the mRNA reads using the MEGAscript T7 kit (Invitrogen, Cat# A57622). The amplified RNA was mixed with ExoSAP-IT PCR reagent (Invitrogen, Cat# 78200.200.UL), fragmented using 200 mM Tris-acetate (pH 8.1), 500 mM KOAc, 150 mM MgOAc, and reverse transcribed into cDNA. Second-strand cDNA were ligated to Illumina sequencing adapters and underwent PCR amplification. DNA sizes were selected with an average of about 400 bp with two 0.8x DNA bead cleanups (AMPure, Cat# A63882). DNA libraries were sequenced using the NovaSeq™ 6000 system (Illumina), and raw reads were normalized and mapped to the mouse reference genome mm10 (GRCm38).[61]

Please cite this article in press as: Bond et al., Prior Fc receptor activation primes macrophages for increased sensitivity to IgG via long-term and short-term mechanisms, Developmental Cell (2024), https://doi.org/10.1016/j.devcel.2024.07.017

CellPress
OPEN ACCESS

Analysis was performed as described in Atkins et al.[55] RNA-seq raw counts were modeled parametrically assuming a negative binomial distribution and p-values were adjusted using the Benjamini and Hochberg method to determine differentially-expressed genes with the *DESeq2* package.[62] The R packages *ashr* and *LIMMA* were used to calculate log fold change shrinkage and remove batch effects, respectively.[63,64] Hierarchical clustering was carried out using *ComplexHeatmap* in R to identify differentially-expressed genes in the dataset and displayed using z-scores.[65]

Gene Ontology analysis was performed on geneontology.org with all differentially expressed genes that met our significance threshold. Only GO terms with a significant false discovery rate <0.05 were displayed.

Kinetics of engulfment

BMDMs were plated as described in the bead engulfment assay 12-24 hours prior to the experiment and stimulated with low intensity LITOS illumination 1 or 12 hours prior to the experiment. Using ND acquisition in Elements, 2-3 positions per well were manually selected. Approximately 4 x 10^5 beads were added and phagocytosis was imaged at 20 s intervals through 7 z planes for 15 min. Only beads that bound within the first 12 min were counted. Bead binding was determined by counting the number of beads bound to cells in the final frame and is shown as a percentage of total beads.

Receptor labeling and single particle tracking

Fab generation

Fabs from rat anti-mouse FcRiii (Cell signaling, Cat# 101307) and rabbit anti-rat biotin conjugated (Invitrogen, Cat# 13-4813-85) were generated using the Pierce Fab Preparation Kit (Thermo, Cat# 44985) according to the manufacturer's protocol. In brief, antibodies were run through a Zeba desalting column to exchange buffers before cleavage with immobilized papain for 3 hours with end over end mixing and digestion was confirmed via SDS-PAGE. Fab fragments were then purified using a NAb Protein A column.

Receptor labeling and imaging

Single FcRs were labeled as previously described.[31] In brief, cells were blocked for 5 min in RPMI supplemented with 5% goat serum. Then, cells were incubated with primary fab fragments for 10 min in blocking medium. Next, cells were incubated with biotinylated secondary fab fragments for 10 min. Finally, cells were washed with blocking media and incubated with streptavidin-conjugated Qdot 655 (Thermo, Cat# Q10123MP) for 4 min and immediately imaged. Images were acquired at 10 fps for 1 min using ND acquisition in Elements on a spinning disc confocal microscope.

Tracking

Tracks and particle mean jump distance were generated using the trackmate plugin on ImageJ.[52,53] Tracks that were less than 50 frames or that contained gaps greater than 3 frames were discarded from analysis. Motion types and diffusion coefficients were determined using moment scaling spectrum analysis using the formula described in Ewers et al.[31,66–68] To characterize each particle trajectory as confined or free, we first calculated the moments of displacement. Let $r_l(n)$ represent the radial position vector of trajectory l, where $n = 0, 1, 2, ..., N_l - 1$ where N_l is the total number of timepoints in the trajectory. The moment of displacement is defined by the following equation:

$$\mu_{\nu,l,\Delta n} = \frac{1}{N_l - \Delta n} \sum_{n=0}^{N_l - \Delta n - 1} |r_l(n+\Delta n) - r_l(n)|^{\nu}$$

Here, μ represents the value of the moment, ν represents the degree of the moment where $\nu = 0,1,2,3,4,5,6$, $|.|$ represents the Euclidean norm and Δn represents the spacing between timepoints where $\Delta n = 0,1,2,...,\frac{N_l}{3}$

Moments for each trajectory l were calculated for each value of ν (each moment) and each value of Δn (every possible timepoint spacing). From prior work, we assume that each moment follows the power shift law $\mu_{\nu}(\Delta n) \propto \Delta n^{\gamma\nu}$ where γ represents the scaling coefficient of moment ν.[69] Scaling coefficients for a moment ν for a trajectory l were found by first performing a linear least squares regression to find the slope of $log(\mu_{\nu,\Delta n})$ vs $log(\Delta n)$. Then, using the power shift law, we used the slope obtained via linear least squares regressions and divided it by the moment ν, with the special case of $\nu = 0, \gamma = 0$, to obtain γ. This special case was added to avoid fitting errors during the next step of our analysis. Once we obtained a γ for each moment ν of a trajectory l, we plotted ν vs. γ and performed a linear least squares regression to obtain the slope of the line formed by ν vs. γ. Calculating and then characterizing each trajectory based off the obtained slope value of ν vs. γ is known as moment scaling spectrum (MSS) analysis and is commonly used to characterize diffusion behaviors for small particles.[66] Near 0 MSS values represent stationary diffusive or confined behavior while MSS values between 0 and 1⁄2 represent subdiffuse or free behavior. We applied these definitions to our MSS values for each trajectory l in order to characterize each trajectory as either confined or free. We were also able to calculate the regular diffusion coefficient for each trajectory using the formula: $D_{\nu=2} = \frac{1}{4}e^{y0}$ where $\nu = 2$ indicates the use of the second moment, also referred to as the Mean Square Displacement (MSD), and y0 is the y-axis intercept for the line formed performing a linear least squares regression on Δn vs $\mu_{\nu=2,l=l,\Delta n}$. All of the code used to perform this analysis is available on GitHub and can be found in the key resources table.

Microscopy

Images were acquired on a spinning disc confocal microscope (Nikon Ti2-E inverted microscope with a Yokogawa CSU-W1 spinning disk unit and an Orca Fusion BT scMos camera) equipped with a 40 × 0.95 NA Plan Apo air and a 100 × 1.49 NA oil immersion

Please cite this article in press as: Bond et al., Prior Fc receptor activation primes macrophages for increased sensitivity to IgG via long-term and short-term mechanisms, Developmental Cell (2024), https://doi.org/10.1016/j.devcel.2024.07.017

objective. The microscope is also equipped with a piezo Z drive and an OkoLabs stage top incubator for temperature, Co2 and humidity control. TIRF imaging was performed with an iLas2 ring TIRF on the same microscope base and same camera. The microscope was controlled using Nikon Elements.

QUANTIFICATION AND STATISTICAL ANALYSIS

Statistical analysis was performed in Prism 8 (GraphPad). The statistical test used is indicated in the relevant figure legend. Sample sizes were predetermined and indicated in the relevant figure legend.